1 OF 1

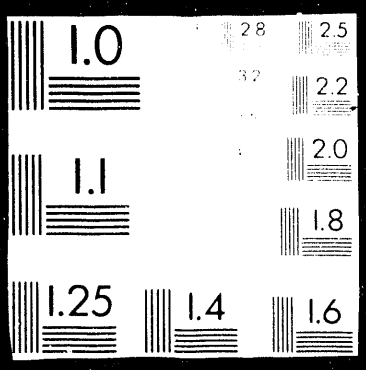

ANL-HEP-TR-90-102

Optimisation Studies For Scintillator Plate Calorimeter

P.K.Job, R.Blair and L.Price

High Energy Physics Division

Argonne National Lab

1. Introduction

This note is the preliminary report of the results of optimisation studies at ANL for the proposed scintillator plate calorimeter for SSC[1]. In this note we have tried to optimise some of the basic parameters for the calorimeter with the available simulation tools at ANL. These simulation studies were carried out using EGS4 and GEANT 3.11(with GHEISHA 7 implementation) on ANL CRAY XMP14 computer. The various input parameters for GEANT and EGS were optimised and validated using the available test beam data. The codes thus validated were used to calculate some of the basic parameters for the scintillator plate calorimeter for SSC with different absorber materials.

2. Validation of GEANT and EGS with test beam data

Test beam data from four different experiments were compared with the results of full shower simulation using GEANT and EGS. Four benchmarks have been chosen so far to compare the test beam results with the simulation.

The benchmarks chosen for this study are

a.ZEUS FCAL Prototype Measurements[2].

b.Bathow's study of EM showers in Lead[3].

c.WA 78 (ZEUS) Experiments, Catanesi et al[4].

d.Iron Scintillator Calorimeter Experiment, Bollini et al[5].

Work supported by the U.S. Department of Energy, Division of High Energy Physics, Contract W-31-109-ENG-38.

DISCLAIMER

2.a ZEUS FCAL Prototype Measurements

The ZEUS FCAL Prototype modules consist of 3.3 mm thick Depleted Uranium and 2.6 mm scintillator plates. Fig.1 gives the experimental set up. The Depleted Uranium plates are clad in 0.2 mm of Stainless Steel. Each module consists of four $20^{*}20^{2}$ cm towers and is segmented longitudinally into an Electromagnetic ($1\lambda_{int}$) Hadronic I ($3\lambda_{int}$) and Hadronic II ($3\lambda_{int}$) sections. This geometry is chosen to optimise the energy cuts used in GEANT and to validate the simulation results.

The major kinetic energy cuts used in GEANT are for hadrons,electrons, neutrons and muons, and also for electron,muon and hadron bremsstrahlung and for delta ray production by electrons and muons. The sensitivity of the shower parameters to these energy cuts is carefully evaluated. The Shower profiles and the energy depositions in the various modules of the calorimeter are estimated for 10 GeV pions for which detailed ZEUS measurements are available[3]. The energy cuts considered are 10 MeV, 5 MeV, 1 MeV,300 KeV and 100 KeV. All the GEANT cuts are set to the same value for both active and absorber material.

Fig.2 gives the total energy deposition in the scintillator plates as a function of all the energy cuts. It can be seen that below the energy cut of 1 MeV, the calculated total energy deposition is not very sensitive to the cuts. But between the energy range of 1 MeV to 10 MeV there is a 20% change in calculated energy deposition. Fig.3 gives the same result as a function of neutron energy cut setting all other cuts as 300 KeV. This also confirms the above conclusion. It can also be inferred that roughly 50% of the error in the GEANT estimation of energy deposition due to higher energy cuts is caused by neutrons in the energy range of 1 MeV to 10 MeV.

The longitudinal shower profiles corresponding to these energy cuts are given in fig.4 and 4a. The shower profiles are normalised to the total energy deposition in the scintillator. The plots show that the differential energy deposition in the scintillator layers is sensitive to the energy cuts even below 1 MeV. Table I gives the comparison of the calculated differential energy deposition in EMC,HAC1 and HAC11 modules with the experimental measurements[3]. The EMC results are given

for different energy cuts. There is a 5% change in EMC energy deposition when the cuts increased from 300KeV to 1 MeV. The result shows that at the energy cut of 300 KeV the the agreement between the calculation and the measurement is quite good. We therefore chose 300 KeV as the energy cuts for all subsequent GEANT calculations.

2.b. Bathow's Measurements in lead

The experimental geometry used by Bathow et al is simulated by EGS code as a rectangular lead block of 20cm*20cm^2 transverse and 22.5 cm (40 radiation lengths) longitudinal dimensions. Fig.5 gives a sketch of the experimental geometry. In the longitudinal direction the geometry was divided into 40 regions (one radiation length each). The energy of the incident beam was 6 GeV with normal incidence on the lead block. The energy deposition was scored for each of these regions. In the transverse direction the energy deposition was scored in 50 bins from the beam position to 5cm (4 Moliere radii). The transverse distributions were obtained at two different shower depths, at 5 and 12 radiation lengths. The number of events simulated were 1000 and the error in energy deposition in each of the longitudinal and transverse bins were evaluated by a separate program. The statistical error in energy deposition is 1.5% at shower maximum and 6% at shower tail.The CPU time utilisation was 0.2 sec/GeV/event on Cray.

The results of this study are given in figs 6,7 and 8. Fig 6 gives the longitudinal shower profile from the simulation plotted along with the experimental profile. The agreement is good. Fig 7 and 8 gives the transverse shower profiles at two different shower depths, at 5 and 12 radiation lengths. A reasonable number of tracks could not be counted beyond 4 Moliere radii. It has also been observed that the transverse profiles are very sensitive to the EGS cut parameters.

2.c.WA 78 DU-Scintillator Calorimeter

The calorimeter consists of 10mm depleted uranium and 5mm plastic Scintillator layers. Fig.9 gives a schematic diagram of the experimental set up. The upstream

uranium part is made of 48 elements consisting of a DU sheet followed by a scintillator sheet. The Uranium is enclosed in 1mm steel.The downstream iron part consists of 58 iron and scintillator elements. The longitudinal shower profiles were measured for Pions in the energy range of 5 to 210 GeV. This geometry is simulated by GEANT. The tail region of iron scintillator calorimeter has not been simulated in this study. Longitudinal shower profiles are obtained for 5, 10, 20, 40 and 135 GeV pions. One thousand events are simulated for each case. The earlier optimised energy cuts of 300 KeV is used for these calculations. The statistical error at each point is less than 4%. The CPU time utilization is 0.1sec/GeV/event on Cray.

The results are given in Figs 10,11,12,13 and 14. It can be seen that the longitudinal shower profiles from GEANT simulation is in reasonably good agreement with the experimental data. GEANT tends to overestimate the energy deposition towards the shower tail. The transverse profiles were not available for comparison.

2.d Iron-Scintillator Calorimeter

This calorimeter consists of iron plates of different thicknesses arranged in a periodic 6-3-6 cm structure. Fig.15 gives the schematic diagram of the experimental set up. Each plate is followed by a plastic scintillator of thickness of 7mm. There were 22 such planes corresponding to a total depth of 120 cm of Iron. The longitudinal and transverse shower profiles were measured for electrons and pions of 20,40 and 86 GeV.

This configuration is simulated by GEANT and EGS. Shower profiles are generated for 40 and 86 GeV pions using GEANT. One thousand events are simulated for each case. The energy cuts used are 300 KeV. The statistical error on each point is less than 5%. The CPU time utilisation is 0.1 sec/GeV/event. The results are given in figs 16 and 17. The agreement is very good.

Inorder to compare the two programs, the EM shower profiles are generated for the same configuration using both GEANT and EGS for 40 and 86 GeV. 500 events are simulated for 40 GeV case and 250 events for 86 GeV case. The error is less than 3%. The CPU time utilisation for GEANT EM shower simulation

is~0.2sec/GeV/event and for EGS ~0.3sec/Gev/event. The results are given in Figs 18 and 19. The agreement is good except at the shower tail where the simulated data are high, this time for EM showers. It can also be noticed that in this case the agreement between EGS and GEANT is excellent.

Our initial evaluation of the results of this study so far is that to first order GEANT and EGS reasonably reproduce test beam profiles and integral energy deposition. For hadronic showers, GEANT some times give longitudinal profiles that are high in the tail region (after about 3 interaction lengths). For electromagnetic showers, the comparison with the data of Bollini,et al., shows EGS giving high results after about 20 radiation lengths. For both hadronic and electromagnetic showers, it would be desirable to have more comparisons with different data sets, in order to separate the shortcomings of the simulations from those of the data. Careful benchmarking is also desirable for resolution and e/h results. Relatively few transverse experimental profiles have yet been found for comparison.

3. Configurations Considered For SSC Calorimeter

The purpose of this study is to evaluate some of the basic parameters for a scintillator plate calorimeter for SSC. Different absorber materials were considered from the point of view of the compensation, resolution and cost. The shower dimensions are evaluated to determine the optimum tower size and the longitudinal shower containment. Response plots are generated to estimate the resolution.

Three configurations are considered in this study,

1. Depleted Uranium- Scintillator
2. Lead- Scintillator
3. Iron- Scintillator

In all cases approximately compensating ratio of thicknesses of absorber and active media are chosen based on the previous studies [6,7,8,9]. The salient features of these configurations are given in Table II. In these preliminary estimates effect of cladding has not been simulated. The earlier optimised GEANT and EGS[10] energy cuts are used.

The the parameters considered for optimisation are

a. The Calorimeter Depth

b. Lateral Segmentation

c. Sampling Thickness

d. e/h Ratio

e. Resolution

3.a Calorimeter Depth

The depth of the calorimeter in terms of the nuclear interaction length of the configuration and its effects on the shower containment and resolution have been studied. This study is carried out for all the configurations and for 10 GeV and 100 GeV pions. The beam is incident in the Z direction at the middle of the tower at normal incidence.

Fig 20 gives the differential energy deposition in the scintillator plates in the DU-SCIN configuration for 10 GeV pions and electrons and Fig 21 gives the integral energy deposition for the same geometry. The average of 500 electromagnetic and 1000 hadronic events are plotted. The Figures show that nearly 98% of the Electromagnetic Shower energy is contained by a thickness of 20 radiation lengths whereas only 20% of the Hadronic Shower energy is contained by the same thickness. This study is extended to determine the total thickness of the calorimeter which can contain a 10/100 GeV hadronic shower. Fig 22 gives the result of this study for the DU-SCIN geometry for both 10 and 100 GeV pions. The shower containment integrated over the radius is plotted as a function of the calorimeter depth in units of nuclear interaction length (λ_{int}). It can be seen that for both the cases a $6\lambda_{int}$ deep calorimeter is sufficient to contain almost 99% of the hadronic shower energy. A $5\lambda_{int}$ thick calorimeter can contain only 92% of the 100 GeV and 95% of 10 GeV hadronic shower.

Fig 23 gives the same result for the three configurations. Almost 98% of the hadronic shower is contained by the calorimeter with a thickness of $6\lambda_{int}$ in all the three cases. In the DU-SCIN case where the ratio of the radiation length to

the nuclear interaction length is the smallest and the sampling is finer in terms of radiation length, the shower is dense and spacially compressed in terms of nuclear interaction length. Therefore the shower containment is the best for DU-SCIN case. This phenomenon is more evident in figure 23.a where the shower containment is plotted in term of calorimeter depth in centimeters. The important practical implication of this result is that one can afford to save on thickness in DU-SCIN case for a fully contained calorimeter.

Fig 24 gives the change in hadronic resolution, $(\sigma/E)_{inf} - (\sigma/E)_t$, as a function of calorimeter thickness (t) at 10 and 100 GeV for DU-SCIN case. The change is plotted with respect to a calorimeter of infinite thickness ($15\lambda_{int}$) on a log scale. The plot fits into an approximate straight line for both 10 and 100 GeV cases. A $6\lambda_{int}$ thick calorimeter has a resolution which is 3% worse than the infinite case for 100 GeV pions and for a $5\lambda_{int}$ calorimeter it is worse by 15%. Fig 25 gives the result of the same study for the three configurations for 10 GeV pions only. The change in resolution is most sensitive to calorimeter depth in the case of DU-SCIN case with one radiation length sampling and least sensitive in the case of Pb-SCIN where the sampling thickness is two radiation lengths.

Both these studies confirm that from the point of view of shower containment and resolution the minimum thickness of the calorimeter must be around 6 interaction lengths for all the three configurations and a thicker calorimeter only improves these parameters marginally.

3.b Lateral Segmentation

The lateral dimensions of the shower profiles are determined accurately to estimate the optimum tower size for the calorimeter. These calculations are done by GEANT binning the lateral energy deposition. Simulations are carried out for all three configurations for 10 Gev and 100 GeV pions. They are also repeated for the proposed projective geometry for 10 GeV case. Fig 26 gives the schematic diagram of the simulated projective tower. The calorimeter is at a radius of 2m from the

interaction point. The longitudinal dimension of the towers is $8\lambda_{int}$ and the outer surface is calculated accordingly.

Fig 27 gives the results of this study for DU-SCIN geometry for 10 GeV and 100 GeV pions. A 10*10 cm^2 tower contains only 50% of the 100 GeV shower whereas a 20*20 cm^2 tower contains more than 75% of the 100 GeV shower. For 10 GeV pions, results are also plotted for both straight and projective towers. For a 20*20 cm^2 projective tower the shower containment improves by 5%. The projective tower improves the shower containment by 15% in the case of 10*10 cm^2 tower. Fig 30 gives the same result for all the three configurations for 10 GeV pions only. The lateral shower containment by towers of Pb-SCIN configuration for 10 GeV pions is very similar to that of DU-SCIN towers. The showers in the FE-SCIN towers, which contains thick iron absorber plates, are fatter in lateral dimensions and requires bigger towers to contain them.

3.c Sampling Thickness

The effect of varying the sampling thickness on the resolution and compensation of the calorimeter is studied using GEANT in the DU-SCIN configuration for 10 GeV pions. The sampling thickness is varied from 1 to 6 radiation lengths.The total depth of the calorimeter is $6\lambda_{int}$ for these calculations.

The change in hadronic and electromagnetic resolution with respect to one radiation length sampling configuration, $(\sigma/E)_{nX0} - (\sigma/E)_{1X0}$, is plotted as a function of the squareroot of the sampling thickness in Fig 29. The results are given for both 10 GeV hadrons and electrons.The Electromagnetic resolution is calculated by EGS and the hadronic resolution by GEANT. The results show that the change in resolution obeys an approximate squareroot law in terms of sampling thickness for both Electromagnetic and hadronic showers upto a sampling thickness of four radiation lengths. Two radiation length sampling worsens the resolution by 6 to 8 % in the case of 10 GeV hadrons and electrons.

Fig 30 gives the e/h ratio calculated by GEANT and EGS as a function of sampling thickness. The value for one radiation length sampling agrees well with ZEUS

measurements[2]. But GEANT estimates of e/h ratio remained insensitive to varying sampling thickness when the ratio of thicknesses of the absorber material to the active material remained same. We feel that this aspect needs further investigation. We are in the process of implementing CALOR code[11] at ANL which is supposed to treat low energy neutron transport better. we have planned an independent estimation of all these parameters using CALOR.

3.d e/h ratio

The e/h ratio for all the three configurations are evaluated using GEANT and EGS and compared with the experimental results. Table III gives the comparison of the results of the calculated e/h ratio for the three configurations with the published experimental results [2][9][14]. The agreement is surprisingly very good. The lower measured value for the ZEUS case could be due to the fact that the cladding is not been simulated which is in the right direction[13]. The agreement of e/h ratio with the measurements in this section and in section 3.c may be fortuous. It can be due to the fact that in the configurations considered, the low energy neutron flux is a slowly varying function of energy and space and the GHEISHA cross sections for low energy neutron transport does not introduce a serious error in the calculated integral energy deposition. However a more detailed e/h evaluation has been planned with CALOR code system which treats the low energy neutron transport $\leq$ 20MeV in 100 lethargy groups and the lethargy group cross sections are obtained by flux weighting the measured point cross section data.

3.e Resolution

Electromagnetic and hadronic resolutions are calculated using EGS and GEANT and compared with the available test beam results. These calculations are done for all the three configurations. The energy range considered is only 5-10 GeV.

EGS results for the DU-SCIN configuration for 5 and 10 GeV electrons are given in Fig.31 and 32. The response plot for 250 events are given for both the cases.

The average and the width at half maximum are estimated by a 2σ fit. The calculated resolutions ($\sigma/\sqrt{E}$) from the fit are given in Table IV along with the ZEUS measurements[13]. The agreement between EGS results and ZEUS measurements for electrons is very good for both the energies. The response plot for PB-SCIN case is given in Fig 33 for 10 GeV electrons .The fitted resolution is given in Table IV. The experimental result[9] is also given for comparison. The agreement is good. It appears that EGS is able to predict the electromagnetic resolution very well for most of the cases although more benchmarking at higher energies for different configurations is desirable.

GEANT results for the DU-SCIN configuration for both 5 and 10 GeV pions are given in Figs 34 and 35. The response plot for thousand events are given. The calculated resolution ($\sigma/\sqrt{E}$) from the fit is given in Table IV along with the measurements[13]. It can seen that the agreement is satisfactory although the simulation data is higher than the measurements. The response plot for PB-SCIN configuration is given in Fig.36 and the fitted resolution in Table IV. The experimental data[9] is given for comparison. The agreement in this case is bad due to some reason we are unable to determine. The response plot for the CDF central hadron calorimeter configuration (FE-SCIN) is given in Fig.37 and 38. The fitted resolutions ($\sigma/\sqrt{E}$) are given in Table IV for 10 and 25 GeV along with the CDF measurements[14]. The agreement in this case is very good.

For all the three configurations estimates of resolution at higher energies (in the range of 50-100 GeV) are needed. Alternate configurations are also to be considered. At present these programs are impeded due to CPU time considerations. Typically a 10 GeV run for 1000 events take roughly an hour on CRAY XMP 14 for all the three configurations. The capability of CALOR in predicting the resolution is also under investigation.

4. Conclusions

The main conclusions of this study can be summarised as follows.

GEANT and EGS reasonably reproduce test beam profiles. But more benchmarking is necessary at higher energies as far as resolution, lateral distribution and e/h ratios are concerned.

The calorimeter depth of $6\lambda_{int}$ is minimum for the full shower containment and a thicker calorimeter only marginally improves the shower containment and resolution. In the case DU-SCIN calorimeters, one can possibly have a saving on thickness.

A 10*10 cm^2 projective tower can contain 75% of the 10GeV shower. This agrees well with ZEUS measurements.

The penalty paid for two radiation length sampling is of the order of 6 to 8% on hadronic and electromagnetic resolution.

The aspect of compensation in terms of two radiation length sampling is to be carefully looked into, preferably by a code like CALOR which simulates low energy neutron transport more accurately.

ACKNOWLEDGEMENTS

The authors wish acknowledge the valuable suggestions given by Dr.J.Proudfoot and Dr.T.Kirk during the progress of this work.

REFERENCES

[1] SSC Subsystem Proposal, ANL-HEP-TR-89-111

[2] E.Ros and T.Tsurugai, ZEUS Note 88-086(1988)

[3] G.Bathow,et. al.,Nucl.Phy.B20(1970).

[4] M.G.Catanesi,et. al.Nucl.Inst.Meth.A260(1987)43-54.

[5] D.Bollini, et al.,Nucl.Inst.Meth.171(1980)237-244.

[6] H.Bruckmann, et al,DESY 86-115(1986).

[7] A.Furtjes, et al,ZEUS 89-69(1989).

[8] R.Wigmans, Nucl.Inst.Meth.A259(1987).

[9] E.Bernadi,et al,Nucl.Inst.Meth.A262(1987)229.

[10] P.K.Job, et al.,Nucl.Instr.Meth.A271(1988)442.

[11] T.Gabriel, et al. CALOR, RSIC Report CCC-178

[12] H.Bruckmann, et al., DESY 87-061(1987).

[13] A.Furtjes, et al.,ZEUS 89-69(1989).

[14] S.Bertolucci, et al.,Nucl.Inst.Meth.A267(1988)301

TABLE I

Comparison with ZEUS FCAL Measurements

Thickness λ	Edep MeV		Edep % 10MeV	Edep % 5MeV	Edep % 1MeV	Edep % 300KeV	Expt. % *(ref 2)*
1	173.6	EMC	37.2±.5	33.1±.5	33.8±.5	36.1±.5	36.7±.1
2	150.5	HAC1				56.7±.5	56.3±.1
3	85.20						
4	37.30						
5	20.10	HAC2				7.2±.5	6.9±.1
6	9.90						
7	4.80						

TABLE II

Salient Features of the Three Configurations

	DU-SCIN	Pb-SCIN	Fe-SCIN
Absorber medium	Depl.Uranium	Lead	Iron
Active medium	Scintillator	Scintillator	Scintillator
Absorber Thickness	0.33 cm	1.00 cm	2.5 cm
Scintillator Thickness	0.26 cm	0.25 cm	1.00 cm
Radiation Length	0.56 cm	0.70 cm	2.42 cm
Nuclear Int. length	17.0 cm	20.3 cm	22.08 cm
Average Density	11.05 gm/cm^3	9.20 gm/cm^3	5.79 gm/cm^3
Global Dimensions	60*60 cm^2	60*60 cm^2	60*60 cm^2

TABLE III

e/h Ratio

	Simu.	Expt.
DU-SCSN	1.03±0.07	1.01±0.04 *(ref 2)*
Pb-SCSN	1.05±0.07	1.05±0.02 *(ref 9)*
Fe-SCSN	1.36±0.10	1.40±0.10 *(ref 14)*

TABLE IV

Comparison of Resolutions

DU-SCIN

	Electrons	*(ref 13)*	Pions	*(ref 13)*
Energy (GeV)	Simu. %	Expt. %	Simu. %	Expt. %
5.0	16.9	17.9±0.2	39.7	34.5±0.5
10.0	16.8	16.5±0.5	37.8	33.2±0.5

PB-SCIN

	Electrons	*(ref 9)*	Pions	*(ref 9)*
Energy (GeV)	Simu. %	Expt. %	Simu. %	Expt. %
10.0	24.9	22.6±0.2	68.8	44.2±1.3

FE-SCIN

	Electrons	*(ref)*	Pions	*(ref 14)*
Energy (GeV)	Simu. %	Expt. %	Simu. %	Expt. %
10.0			66.3	69.5±3.0
25.0			64.5	70.0±3.0

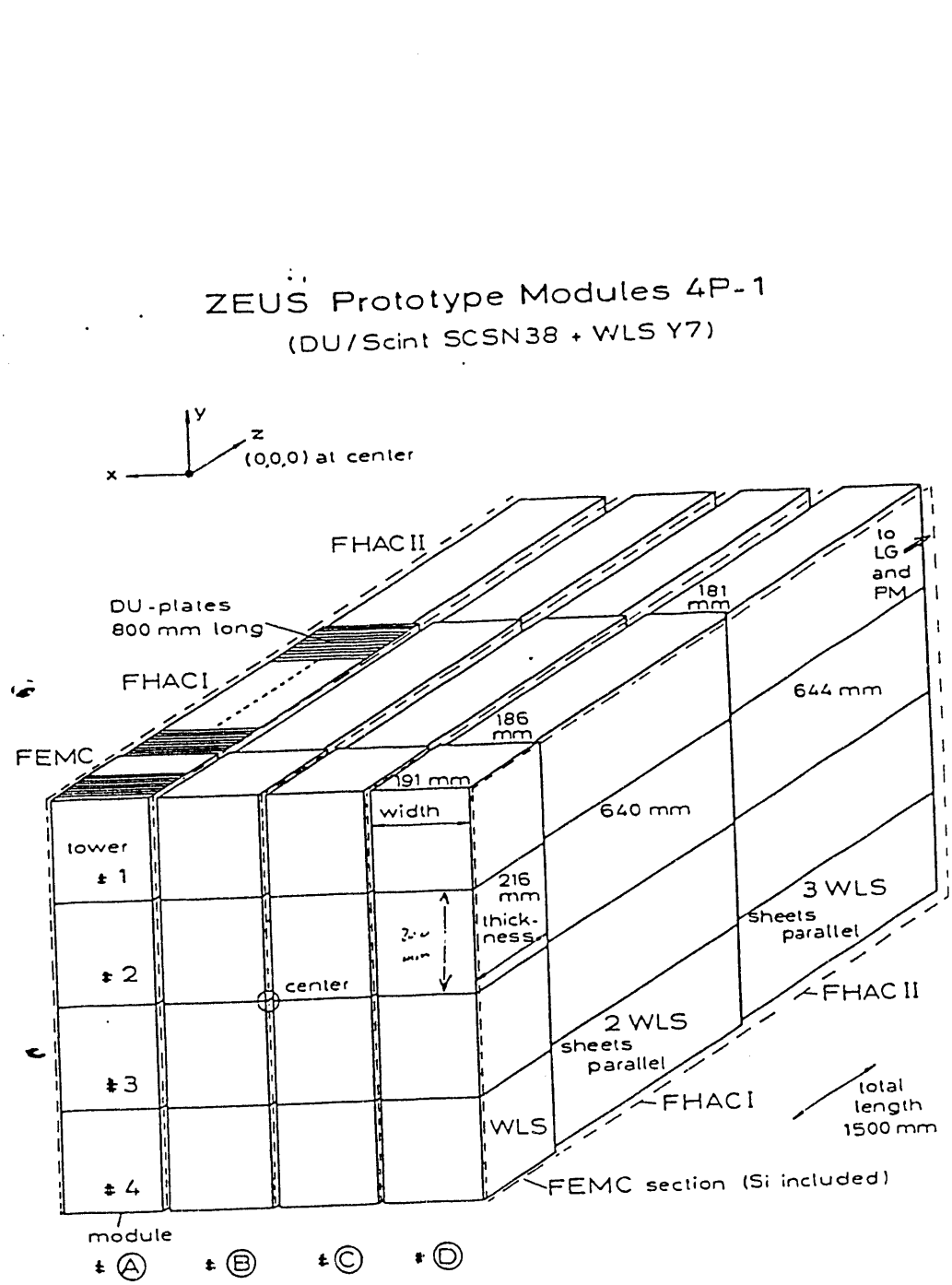
ZEUS Prototype Modules 4P-1
(DU/Scint SCSN38 + WLS Y7)
y
z
x
(0,0,0) at center
FHAC II
DU-plates
800 mm long
FHAC I
FEMC
to
LG
and
PM
181
mm
644 mm
186
mm
191 mm
width
640 mm
lower
± 1
216
mm
thick-
ness
3 WLS
sheets
parallel
± 2
center
FHAC II
2 WLS
sheets
parallel
± 3
FHAC I
total
length
1500 mm
WLS
± 4
FEMC section (Si included)
module
± A
± B
± C
± D

FIG .1

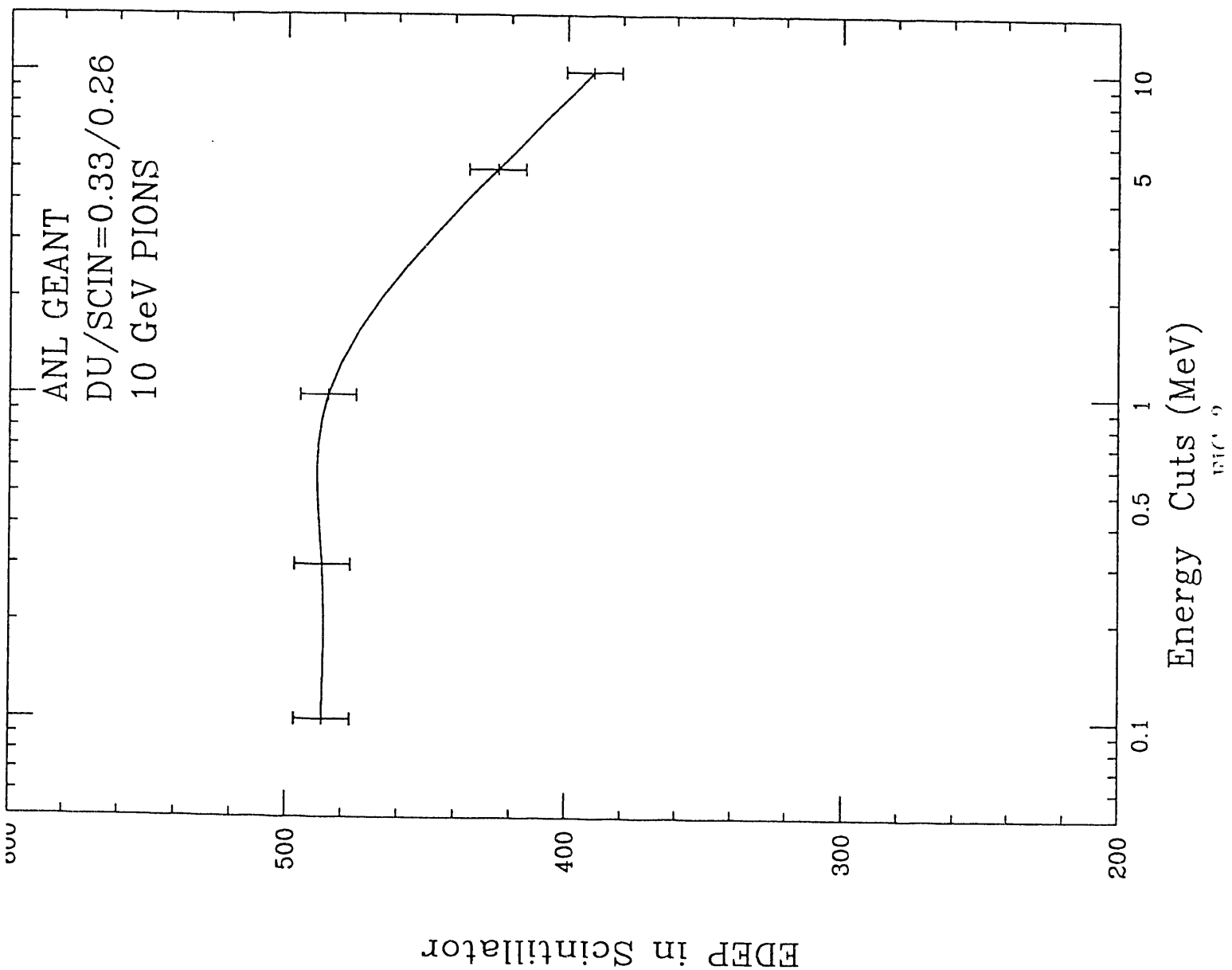
ANL GEANT
DU/SCIN=0.33/0.26
10 GeV PIONS
EDEP in Scintillator
500
400
300
200
0.1
0.5
1
5
10
Energy Cuts (MeV)

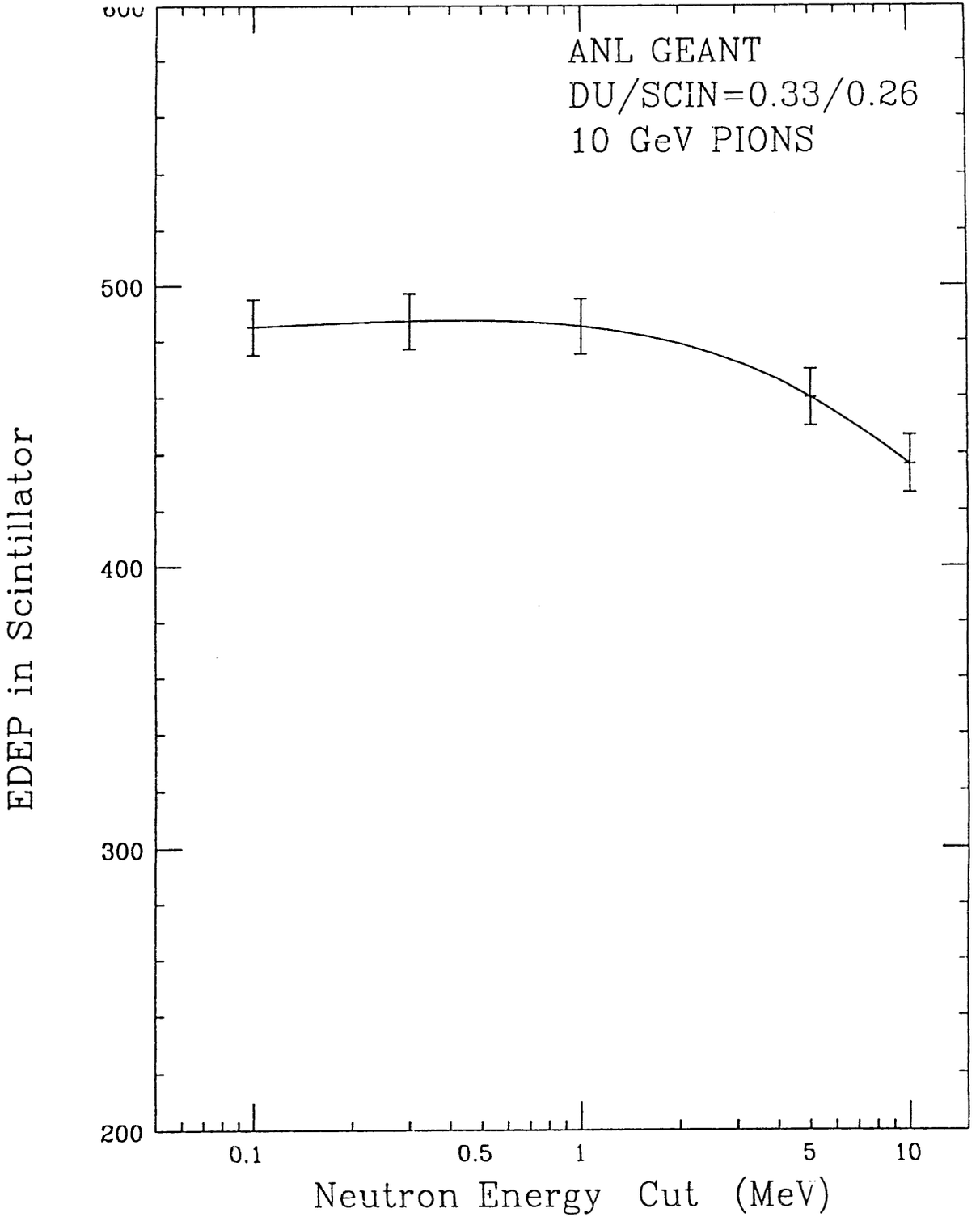
ANL GEANT
DU/SCIN=0.33/0.26
10 GeV PIONS
EDEP in Scintillator
500
400
300
200
0.1
0.5
1
5
10
Neutron Energy Cut (MeV)

FIG .3

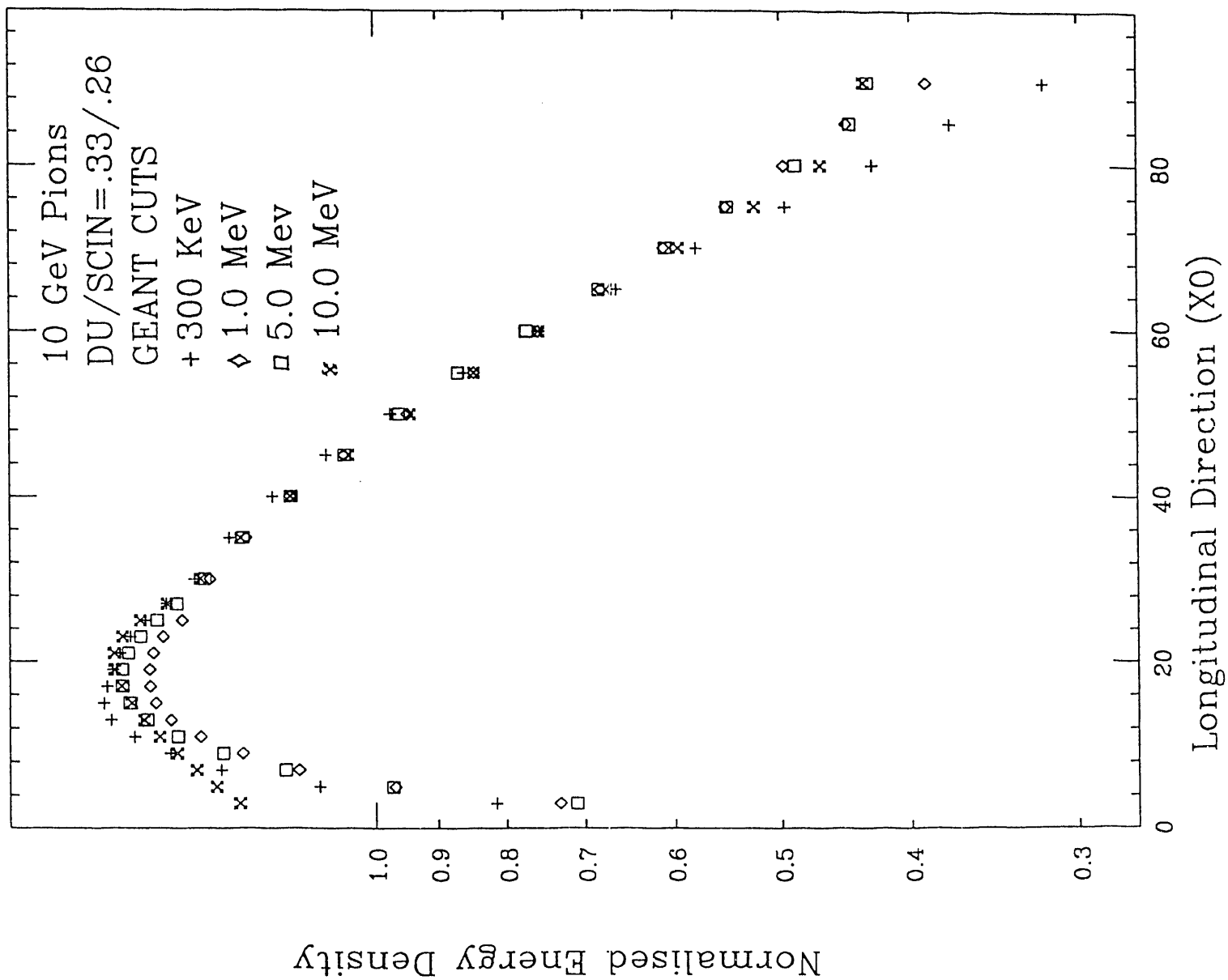
10 GeV Pions
DU/SCIN=.33/.26
GEANT CUTS
+ 300 KeV
◇ 1.0 MeV
□ 5.0 Mev
⊠ 10.0 MeV
Normalised Energy Density
1.0
0.9
0.8
0.7
0.6
0.5
0.4
0.3
0
20
40
60
80
Longitudinal Direction (X0)

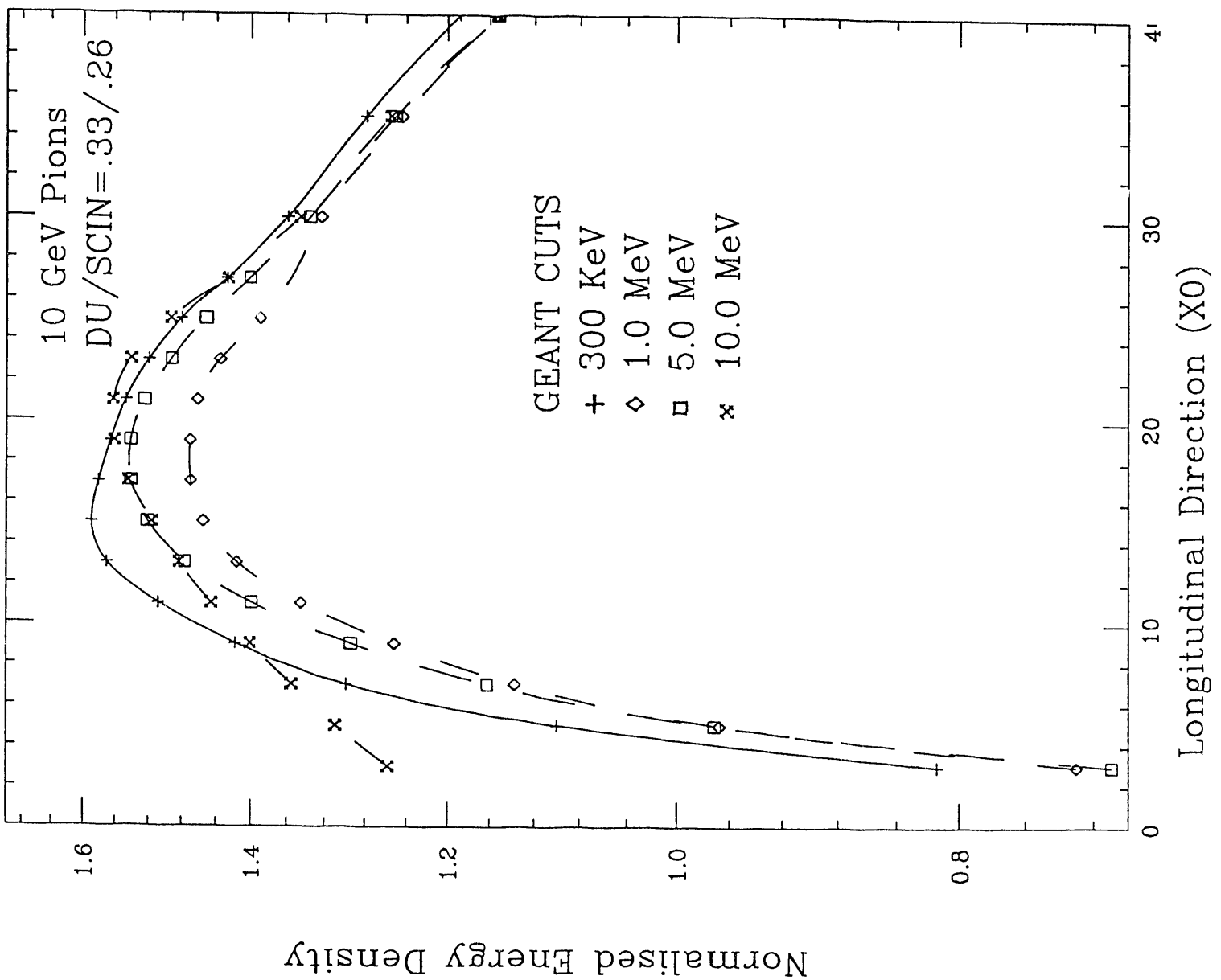
10 GeV Pions
DU/SCIN=.33/.26
GEANT CUTS
+ 300 KeV
◇ 1.0 MeV
□ 5.0 MeV
× 10.0 MeV
Normalised Energy Density
Longitudinal Direction (X0)
0.8
1.0
1.2
1.4
1.6
0
10
20
30
40

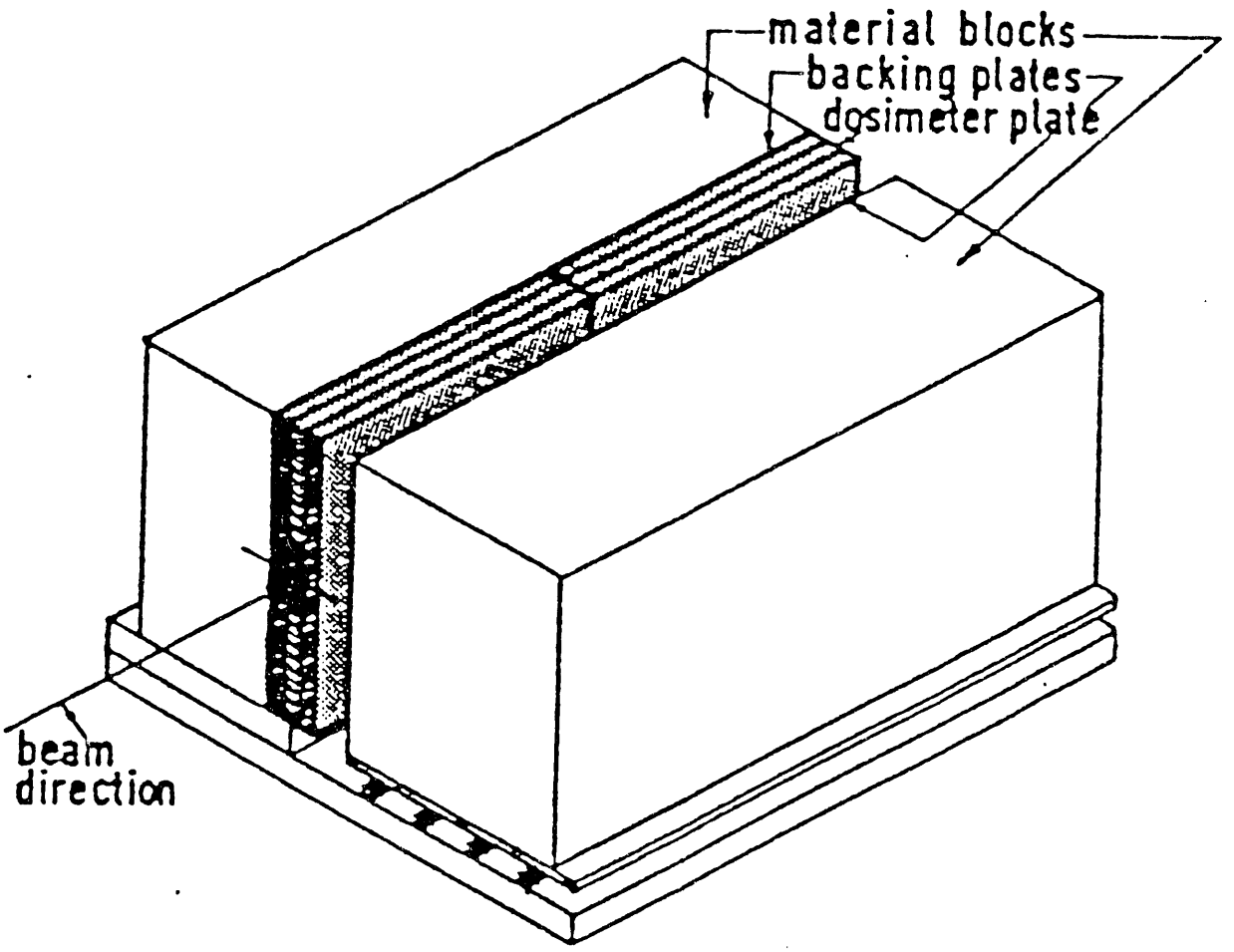
material blocks
backing plates
dosimeter plate
beam
direction

FIG .5

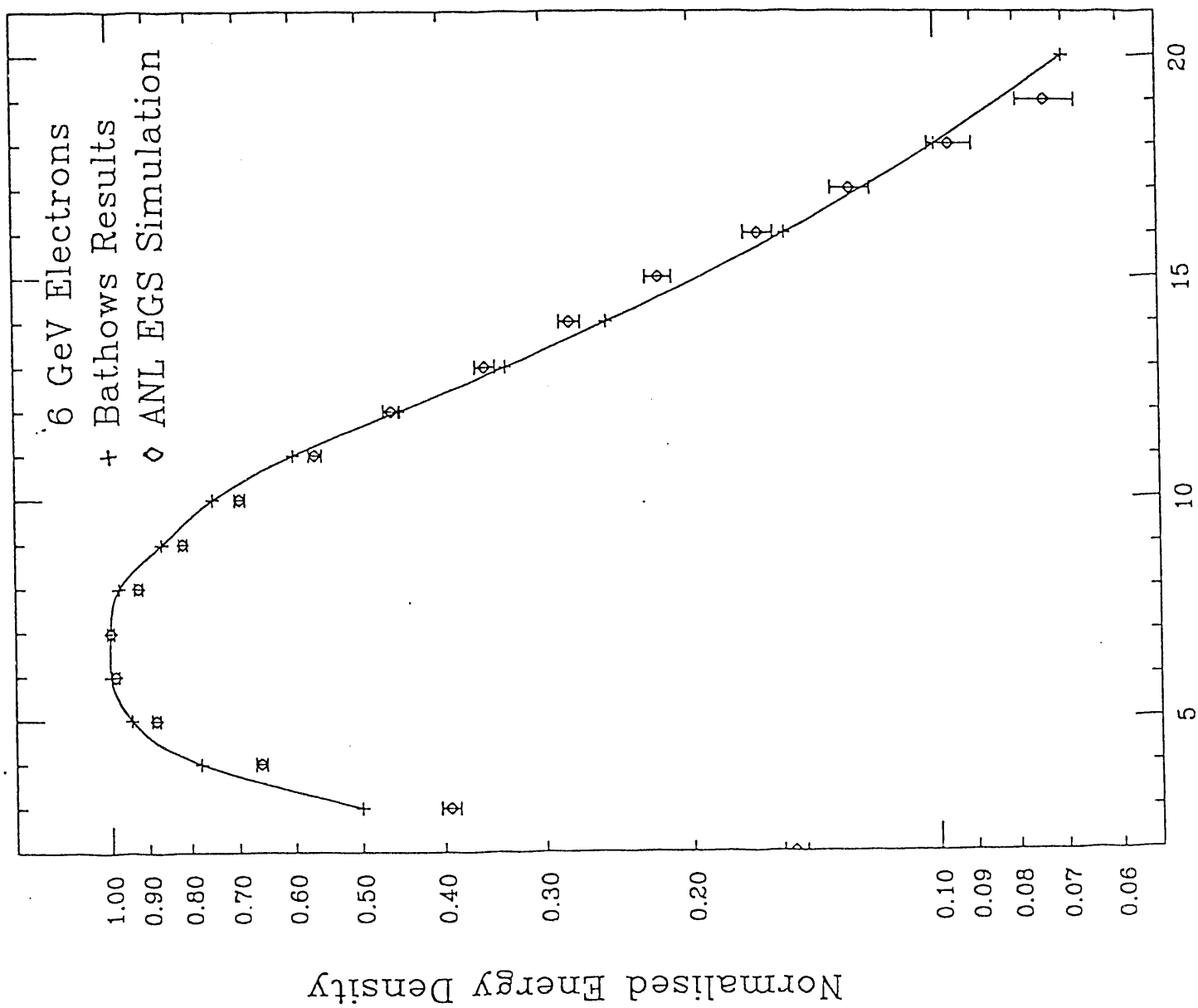
6 GeV Electrons
+ Bathows Results
◇ ANL EGS Simulation
Normalised Energy Density
1.00
0.90
0.80
0.70
0.60
0.50
0.40
0.30
0.20
0.10
0.09
0.08
0.07
0.06
5
10
15
20
Longitudinal Direction (rl)

FIG 6

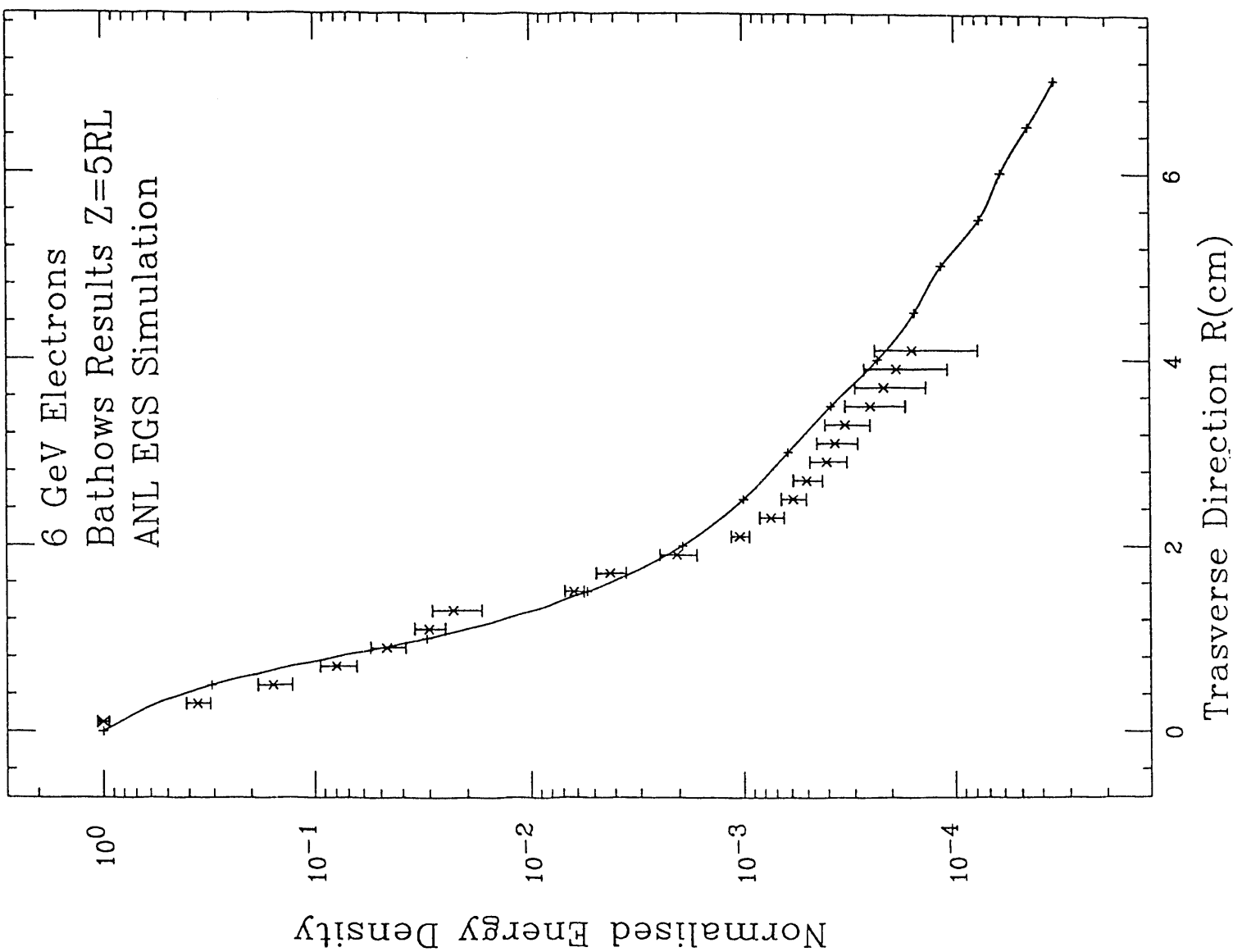
6 GeV Electrons
Bathows Results Z=5RL
ANL EGS Simulation
Normalised Energy Density
10^0
10^{-1}
10^{-2}
10^{-3}
10^{-4}
0
2
4
6
Trasverse Direction R(cm)

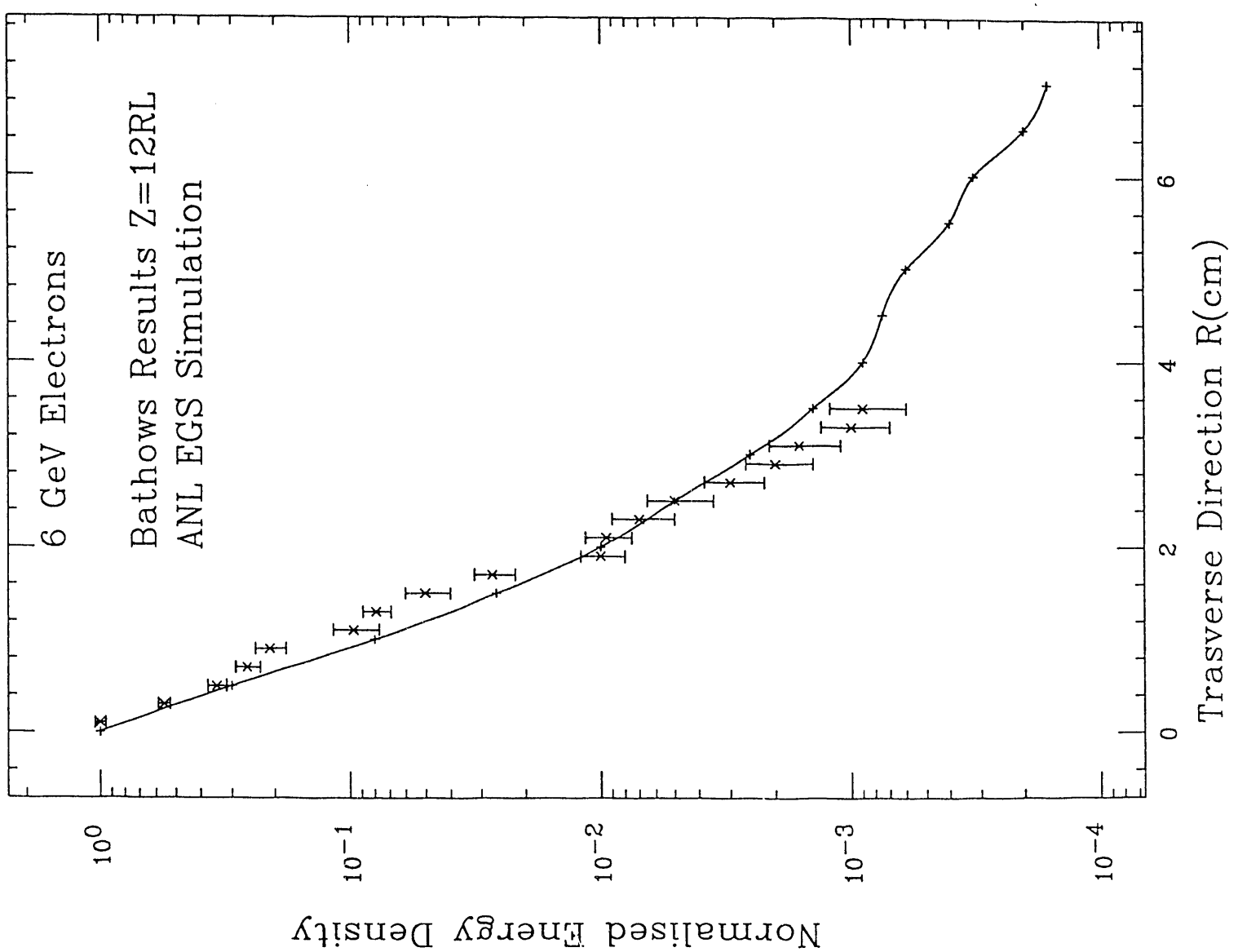
6 GeV Electrons
Bathows Results Z=12RL
ANL EGS Simulation
Normalised Energy Density
Trasverse Direction R(cm)
10^0
10^{-1}
10^{-2}
10^{-3}
10^{-4}
0
2
4
6

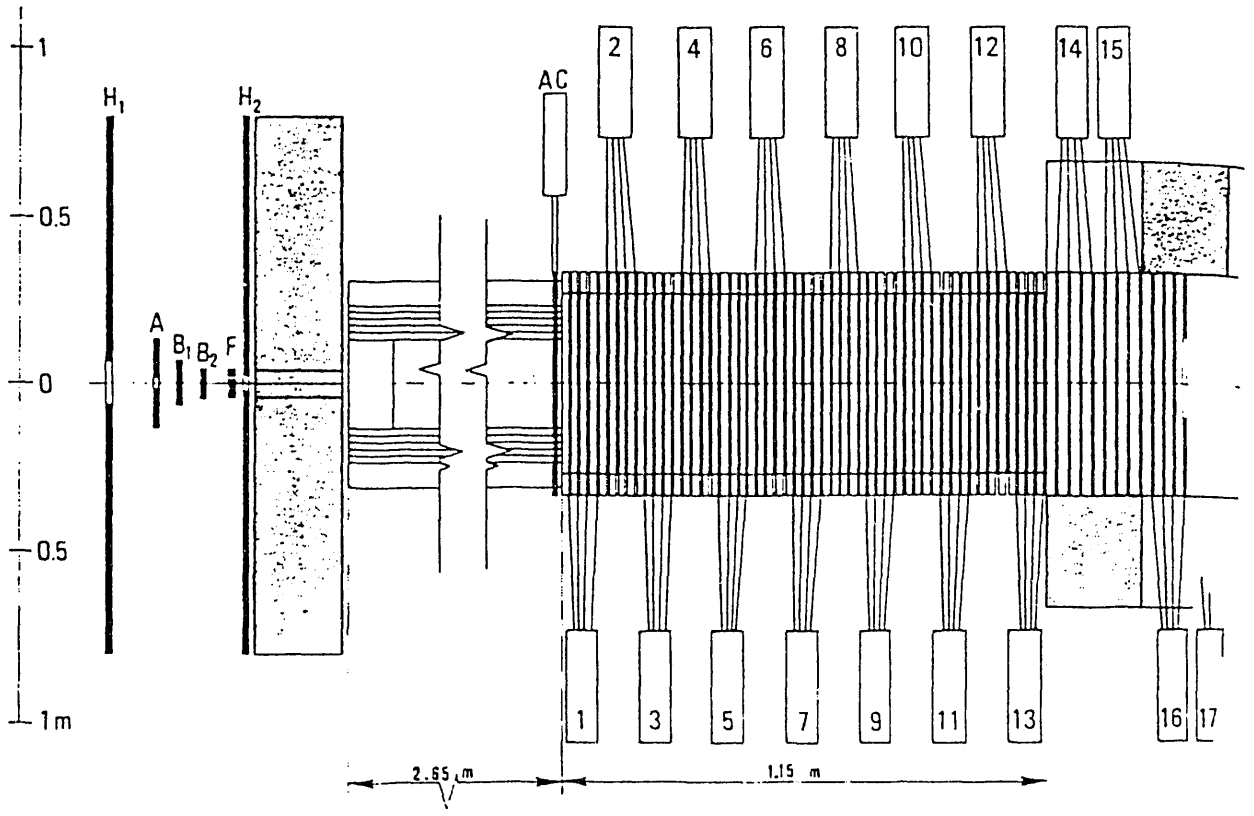
1
0.5
0
0.5
1 m
H1
H2
A
B1
B2
F
AC
2
4
6
8
10
12
14
15
1
3
5
7
9
11
13
16
17
2.65 m
1.15 m

FIG .9

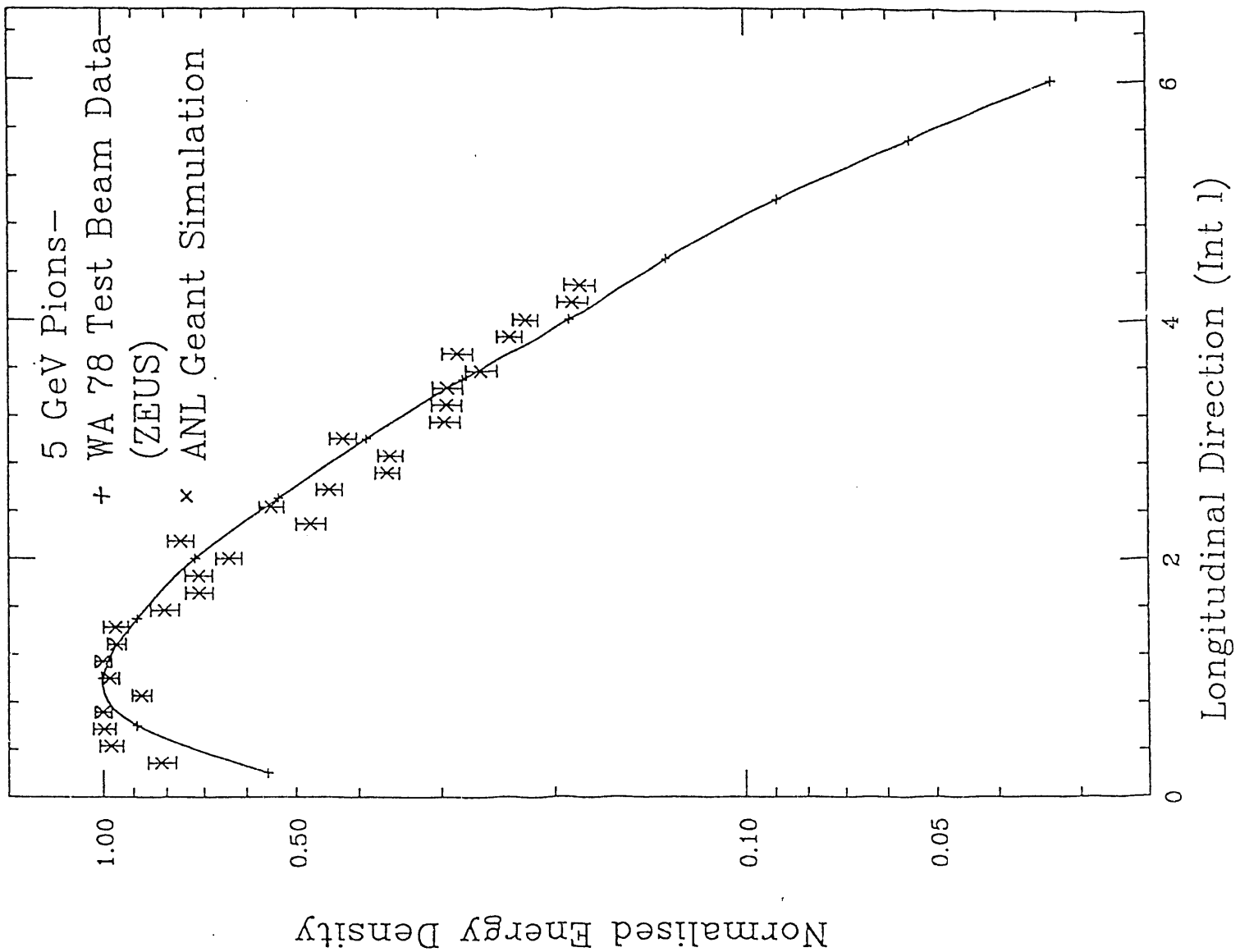
5 GeV Pions—
+ WA 78 Test Beam Data—
(ZEUS)
× ANL Geant Simulation
Normalised Energy Density
1.00
0.50
0.10
0.05
0
2
4
6
Longitudinal Direction (Int l)

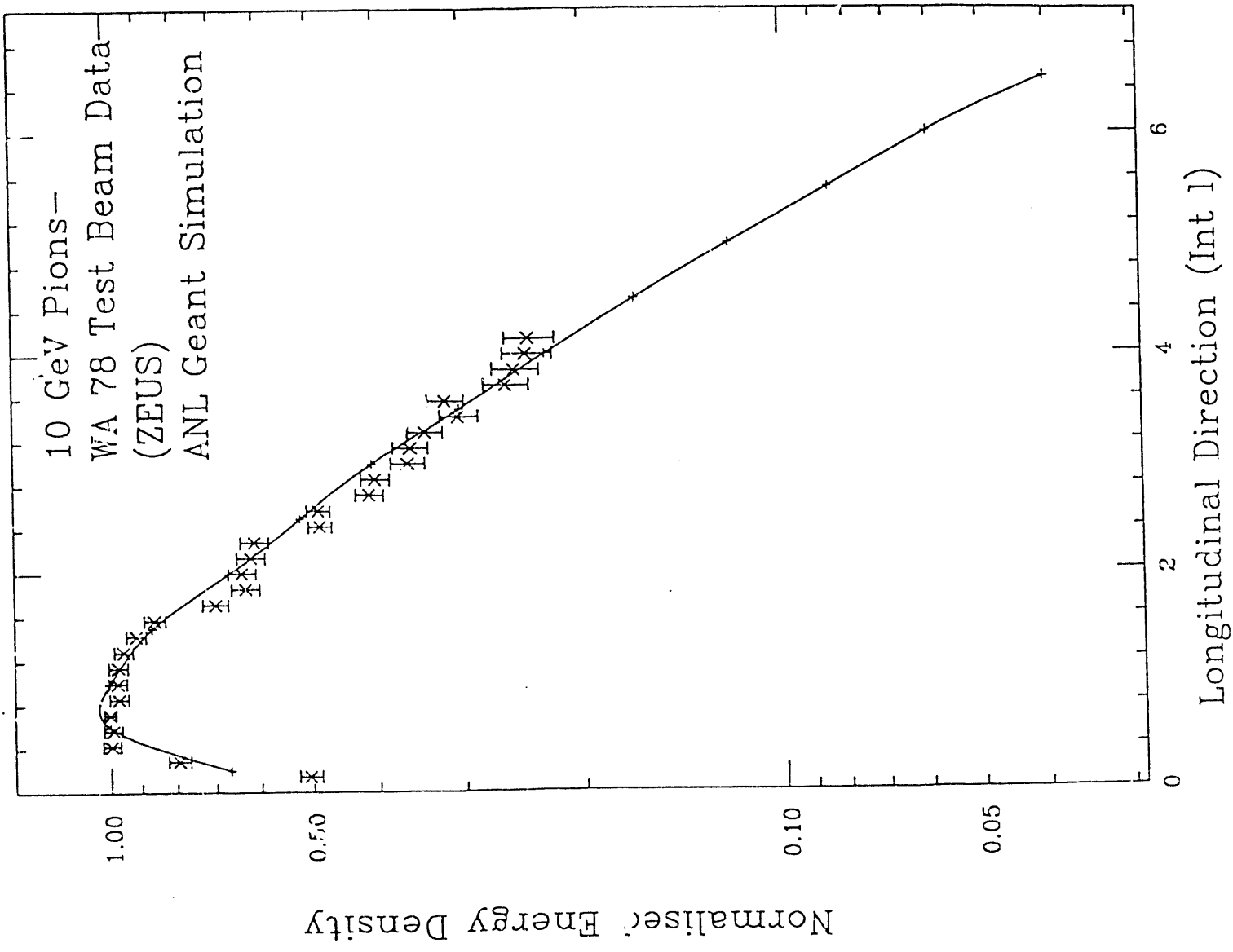
10 GeV Pions—
WA 78 Test Beam Data
(ZEUS)
ANL Geant Simulation
Normalised Energy Density
1.00
0.50
0.10
0.05
0
2
4
6
Longitudinal Direction (Int l)

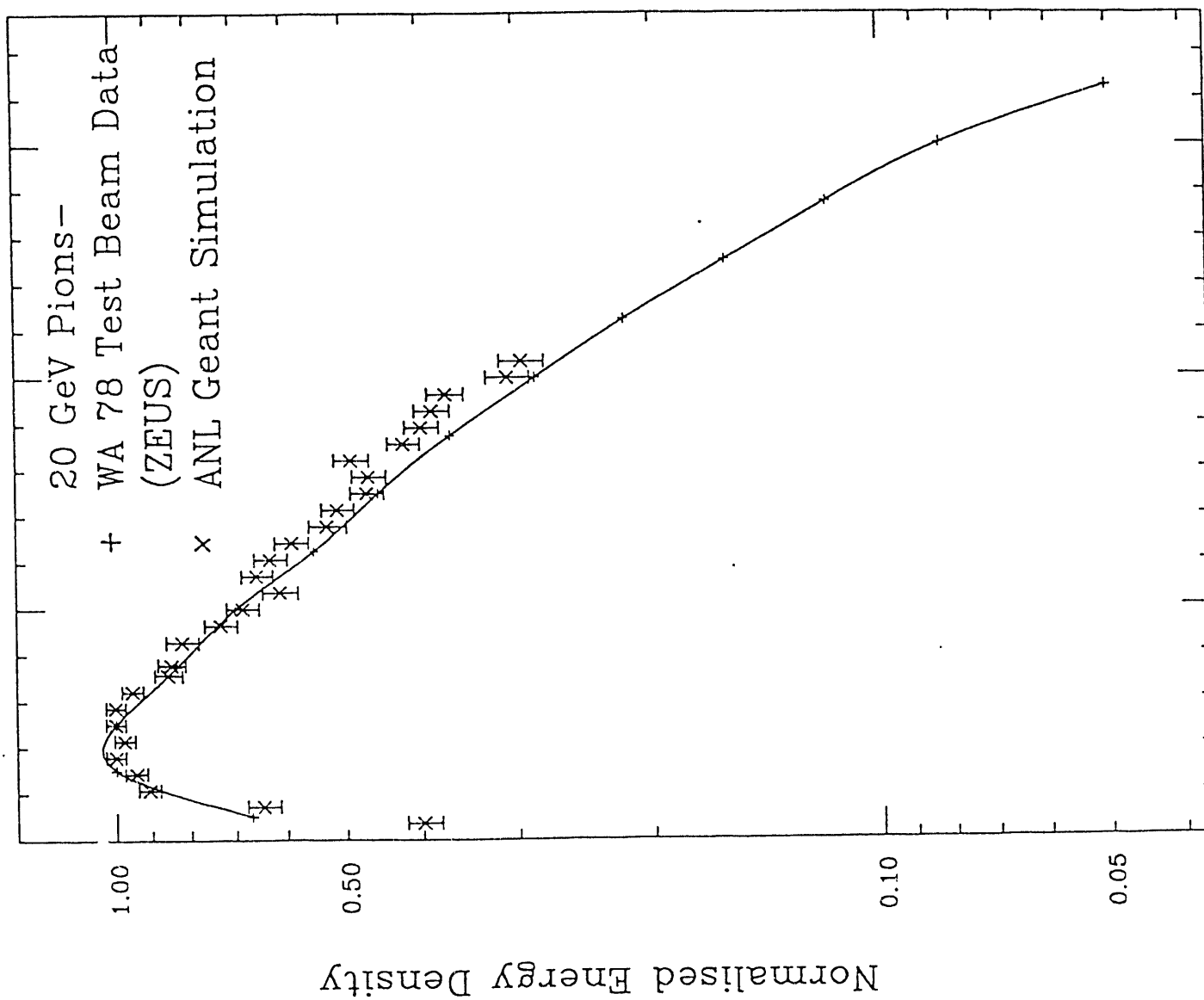
20 GeV Pions-
+ WA 78 Test Beam Data (ZEUS)
× ANL Geant Simulation
Normalised Energy Density
1.00
0.50
0.10
0.05
0
2
4
6
Longitudinal Direction (Int l)

FIG. 19

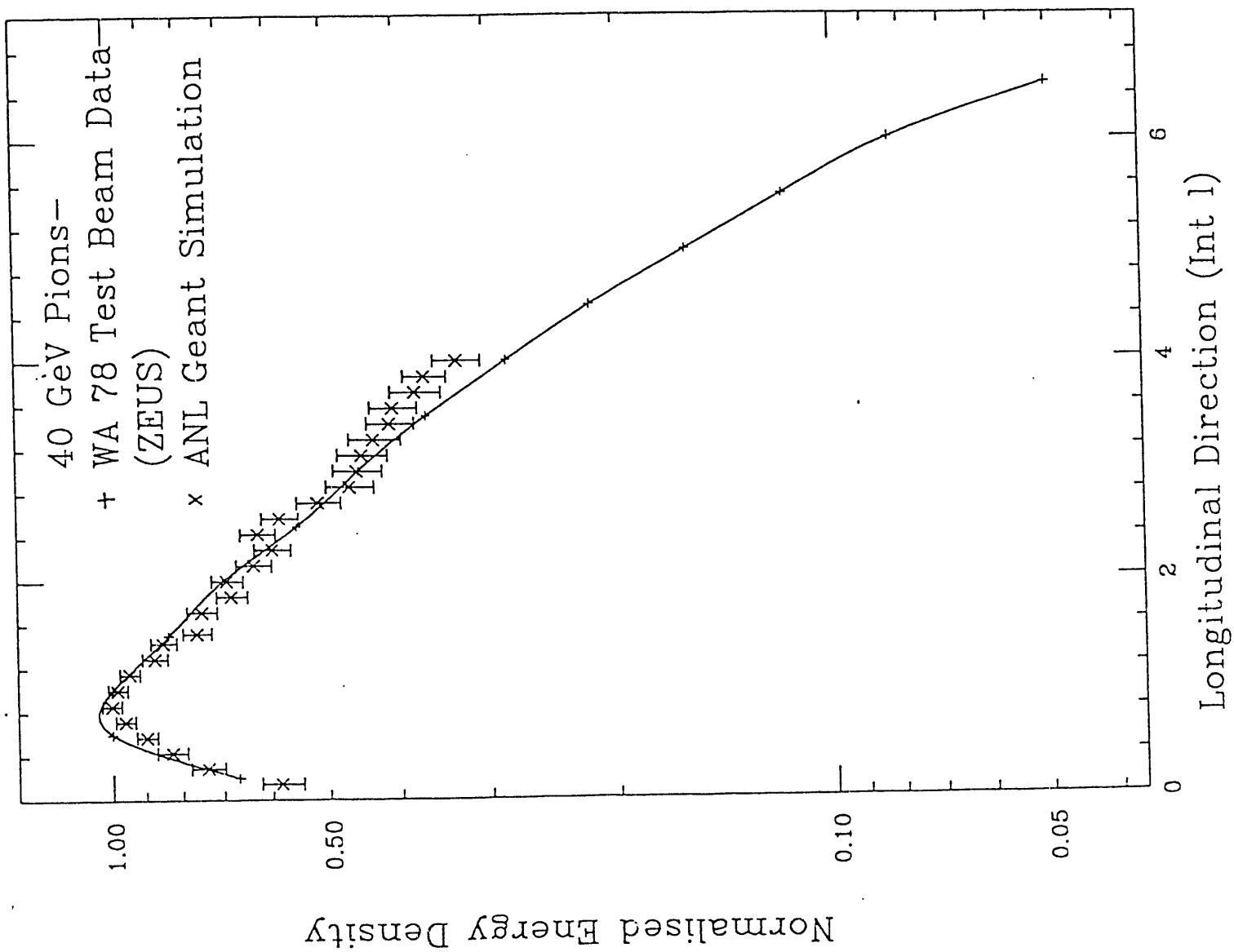
40 GeV Pions−
+ WA 78 Test Beam Data
(ZEUS)
× ANL Geant Simulation
Normalised Energy Density
1.00
0.50
0.10
0.05
0
2
4
6
Longitudinal Direction (Int l)

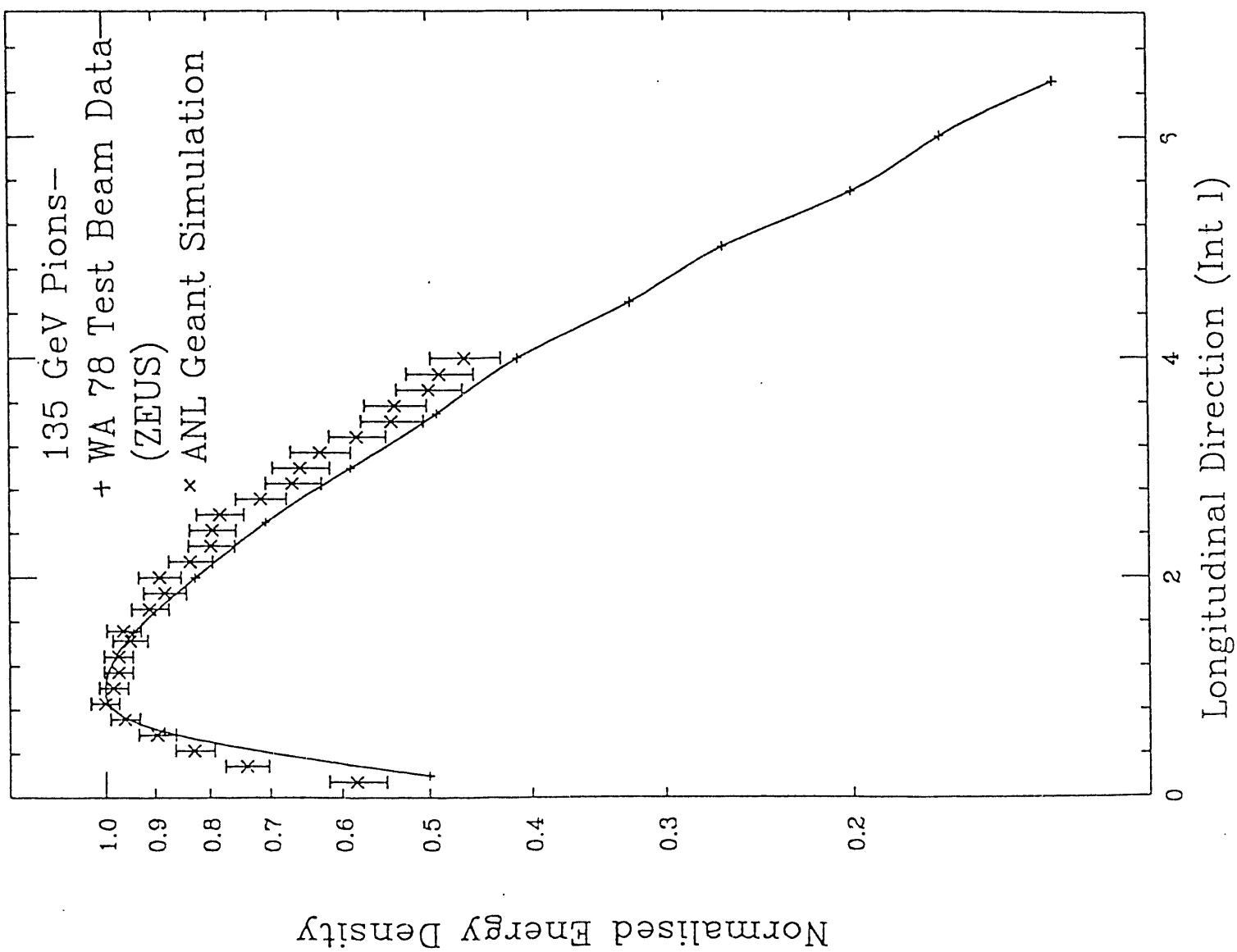
135 GeV Pions—
+ WA 78 Test Beam Data—
(ZEUS)
× ANL Geant Simulation
Normalised Energy Density
1.0
0.9
0.8
0.7
0.6
0.5
0.4
0.3
0.2
0
2
4
6
Longitudinal Direction (Int l)

D. Bollini et al. / An iron-scintillator calorimeter

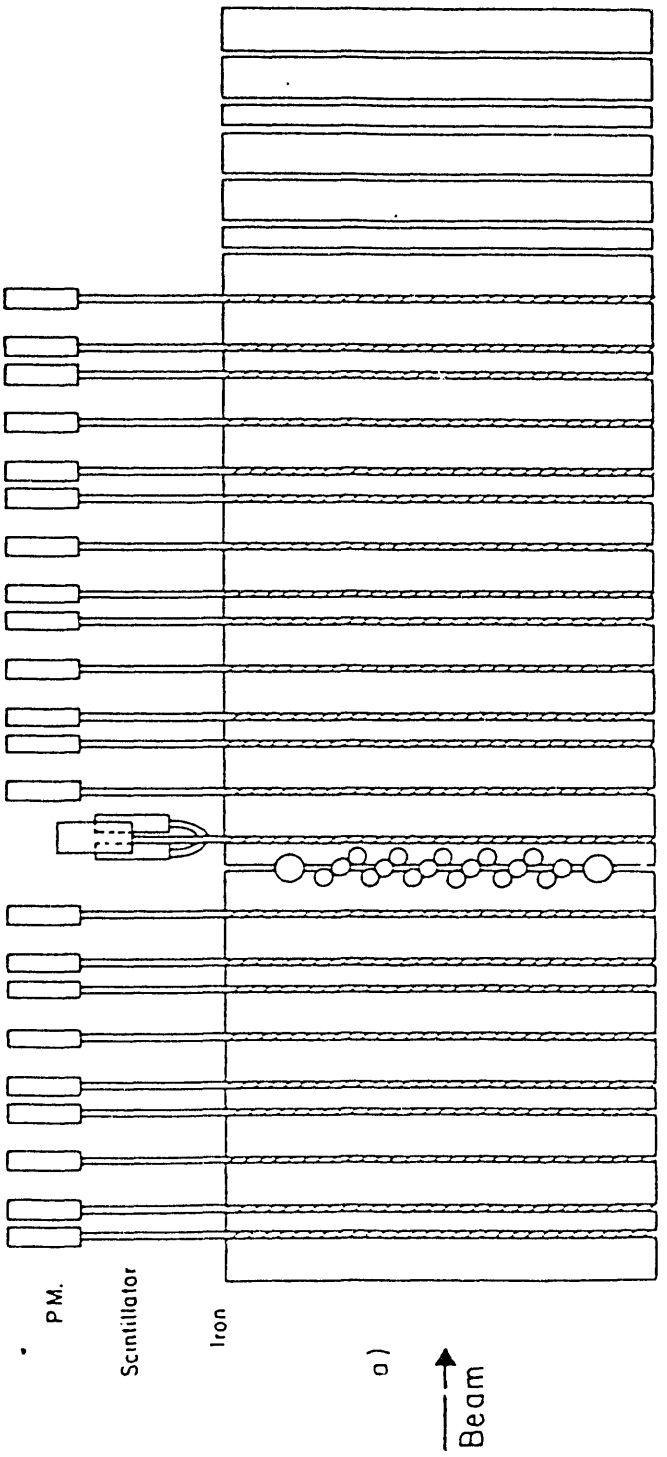

FIG .15

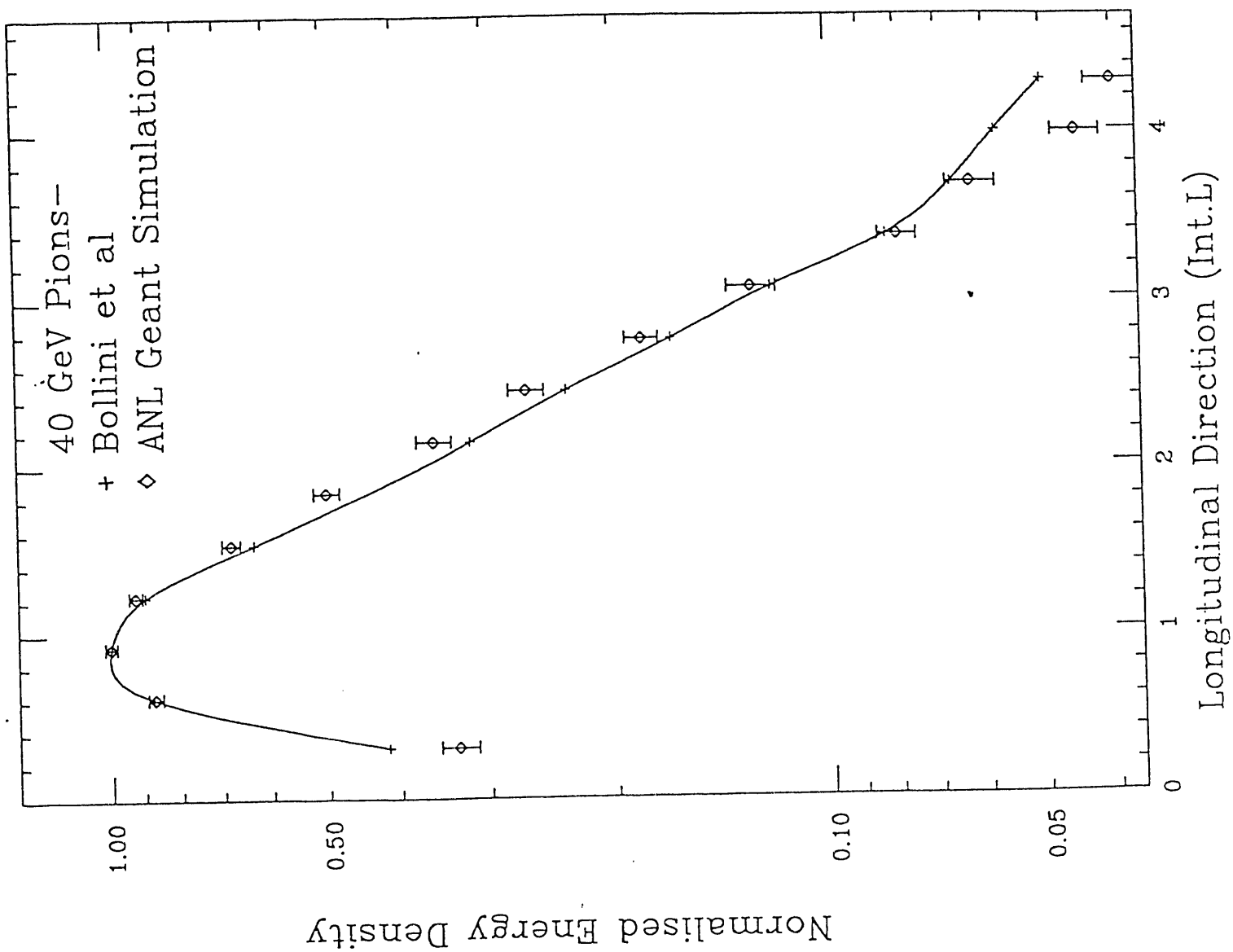
40 GeV Pions-
+ Bollini et al
◇ ANL Geant Simulation
Normalised Energy Density
1.00
0.50
0.10
0.05
0
1
2
3
4
Longitudinal Direction (Int.L)

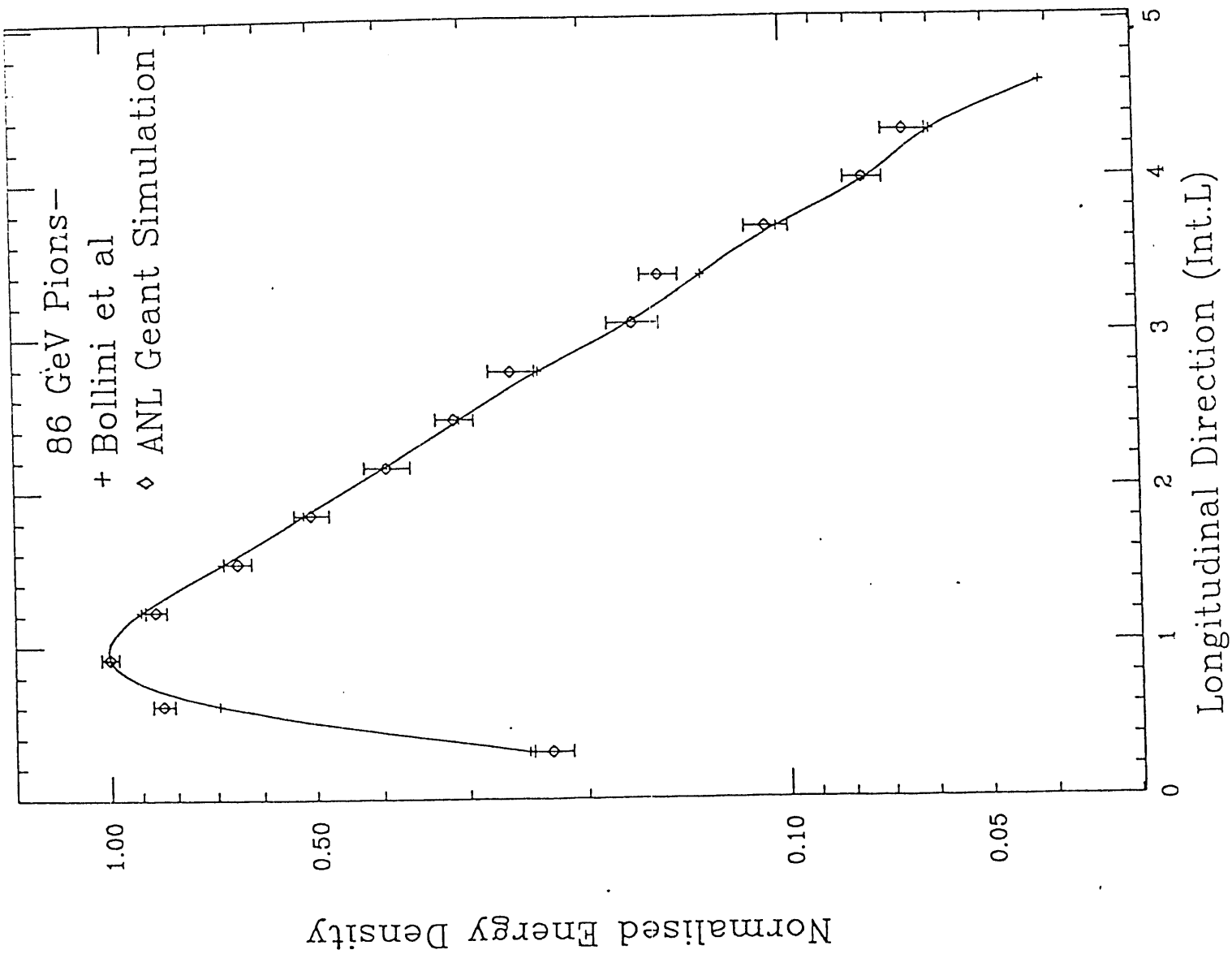
86 GeV Pions-
+ Bollini et al
◇ ANL Geant Simulation
Normalised Energy Density
1.00
0.50
0.10
0.05
0
1
2
3
4
5
Longitudinal Direction (Int.L)

FIG.17

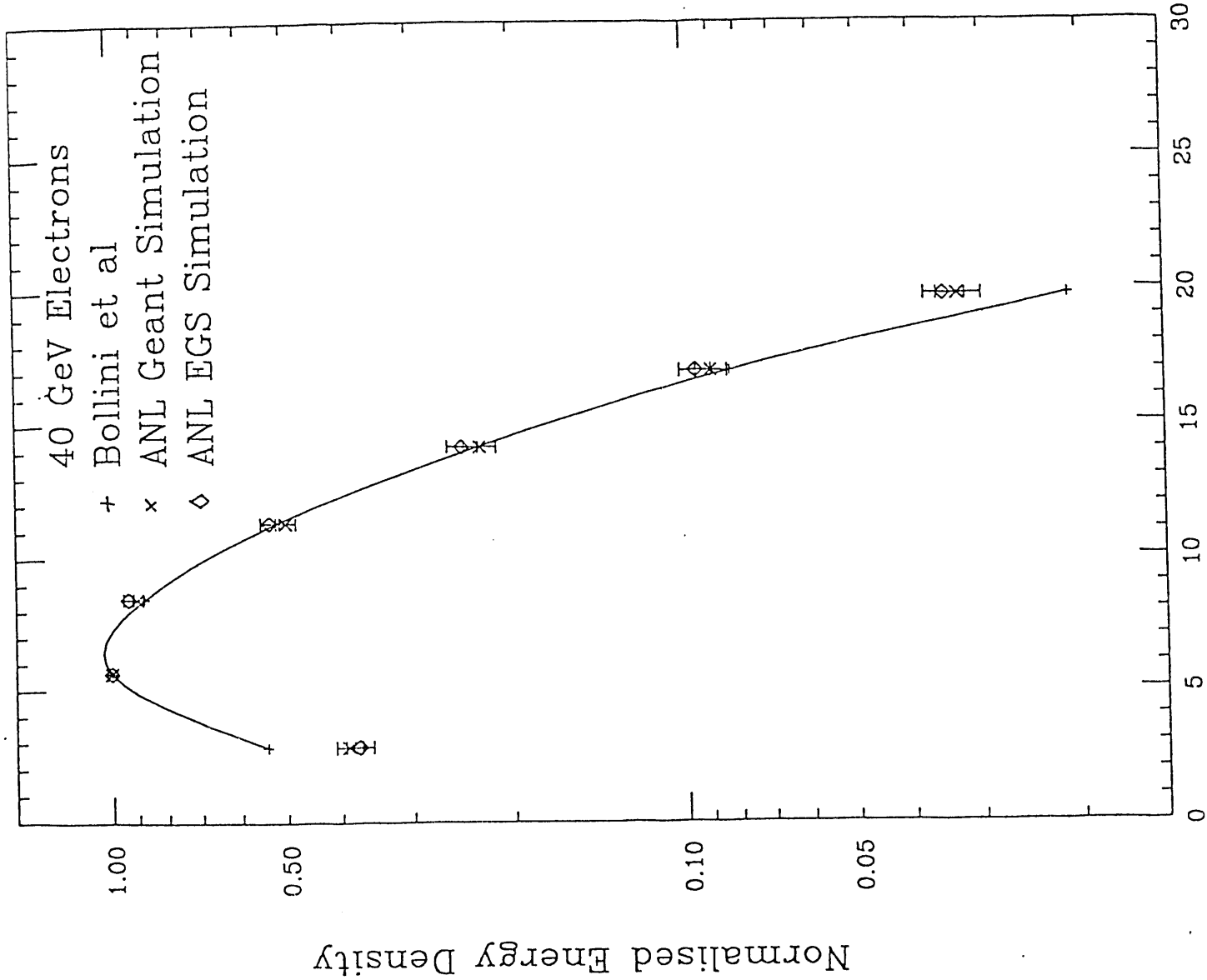
40 GeV Electrons
+ Bollini et al
× ANL Geant Simulation
◇ ANL EGS Simulation
Normalised Energy Density
1.00
0.50
0.10
0.05
0
5
10
15
20
25
30
Longitudinal Direction (rl)

FIG .18

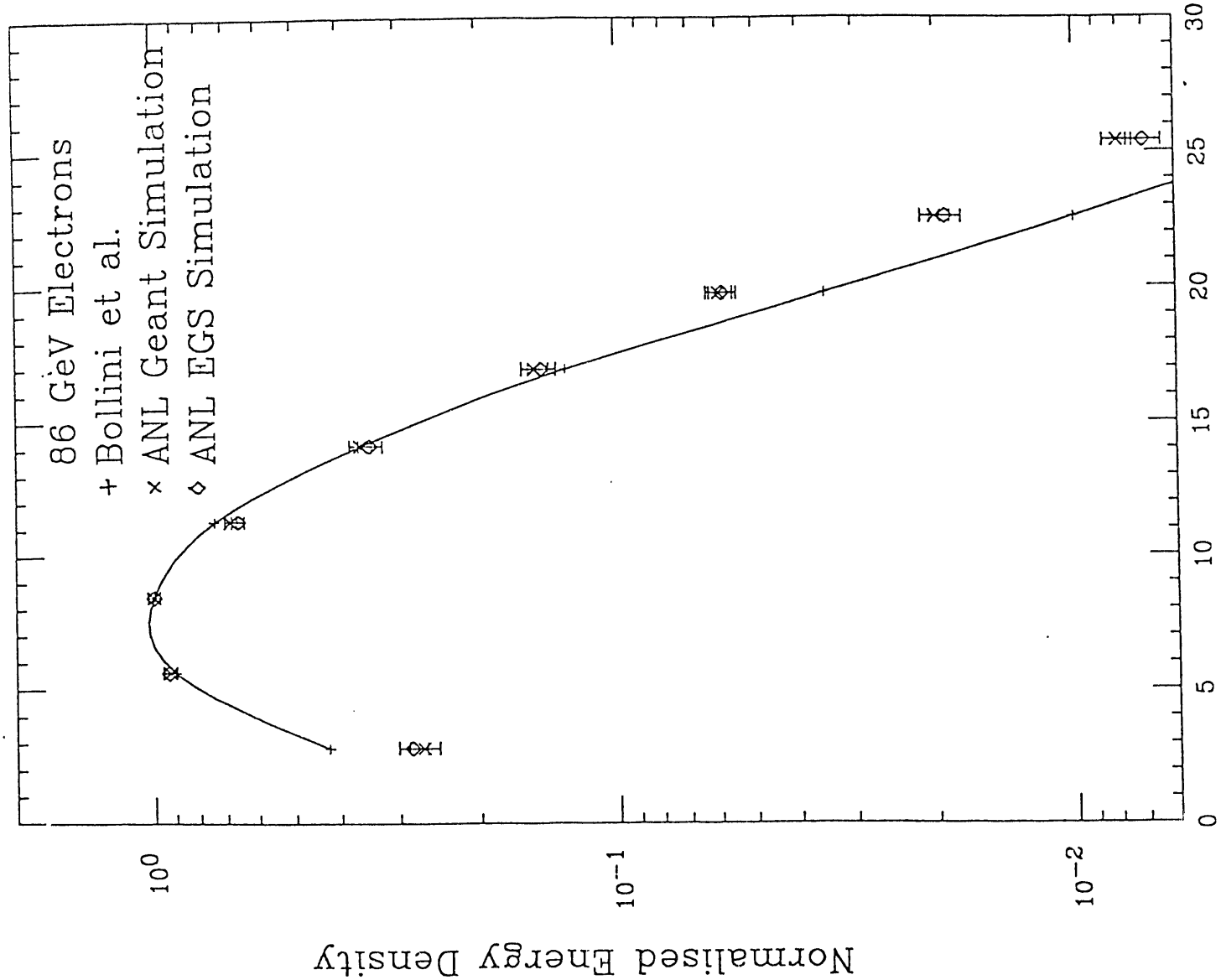
86 GeV Electrons
+ Bollini et al.
× ANL Geant Simulation
◇ ANL EGS Simulation
Normalised Energy Density
10^0
10^{-1}
10^{-2}
0
5
10
15
20
25
30
Longitudinal Direction (rl)

FIG .19

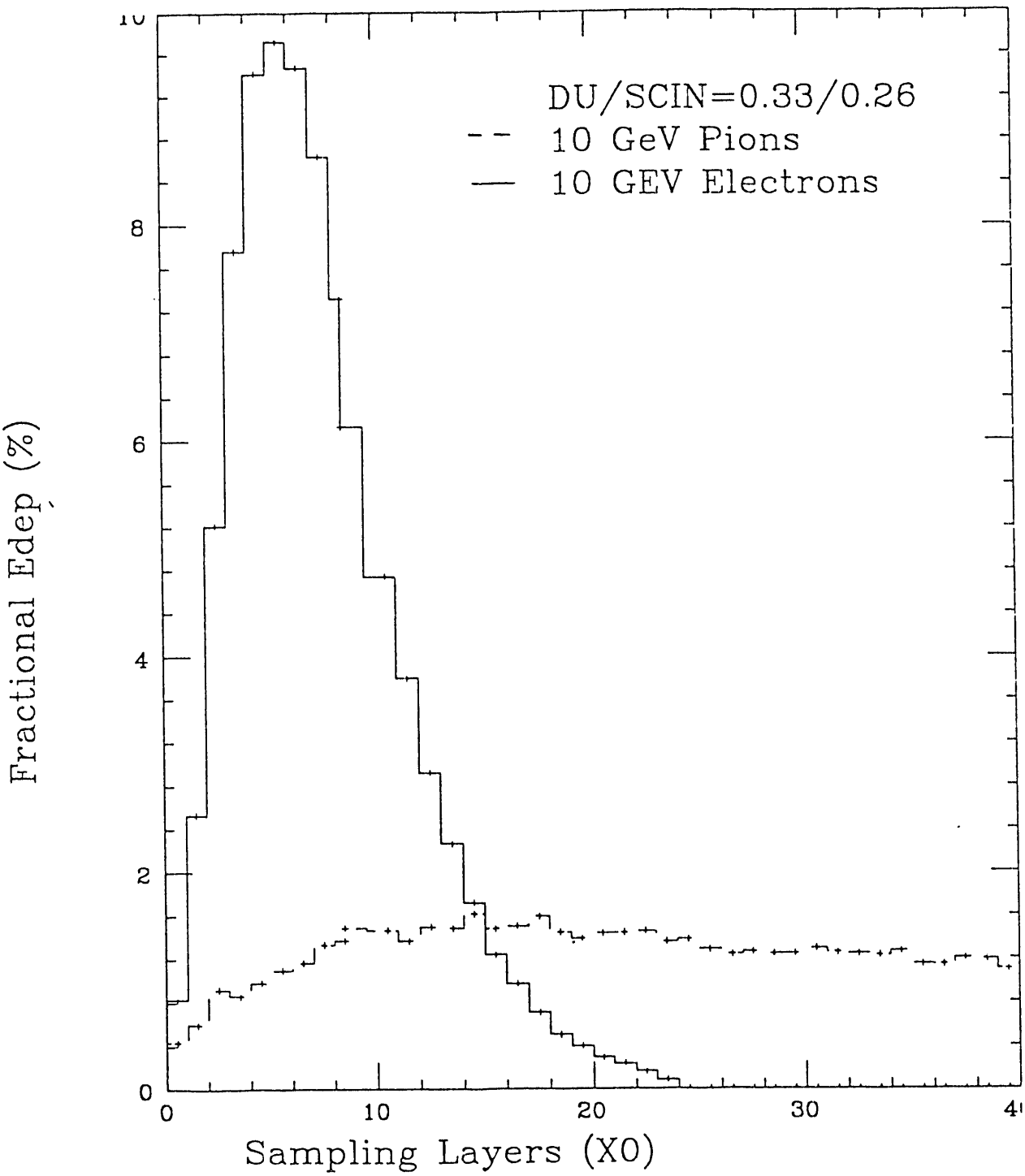
DU/SCIN=0.33/0.26
10 GeV Pions
10 GEV Electrons
Fractional Edep (%)
Sampling Layers (X0)
0
2
4
6
8
10
0
10
20
30
40

FIG .20

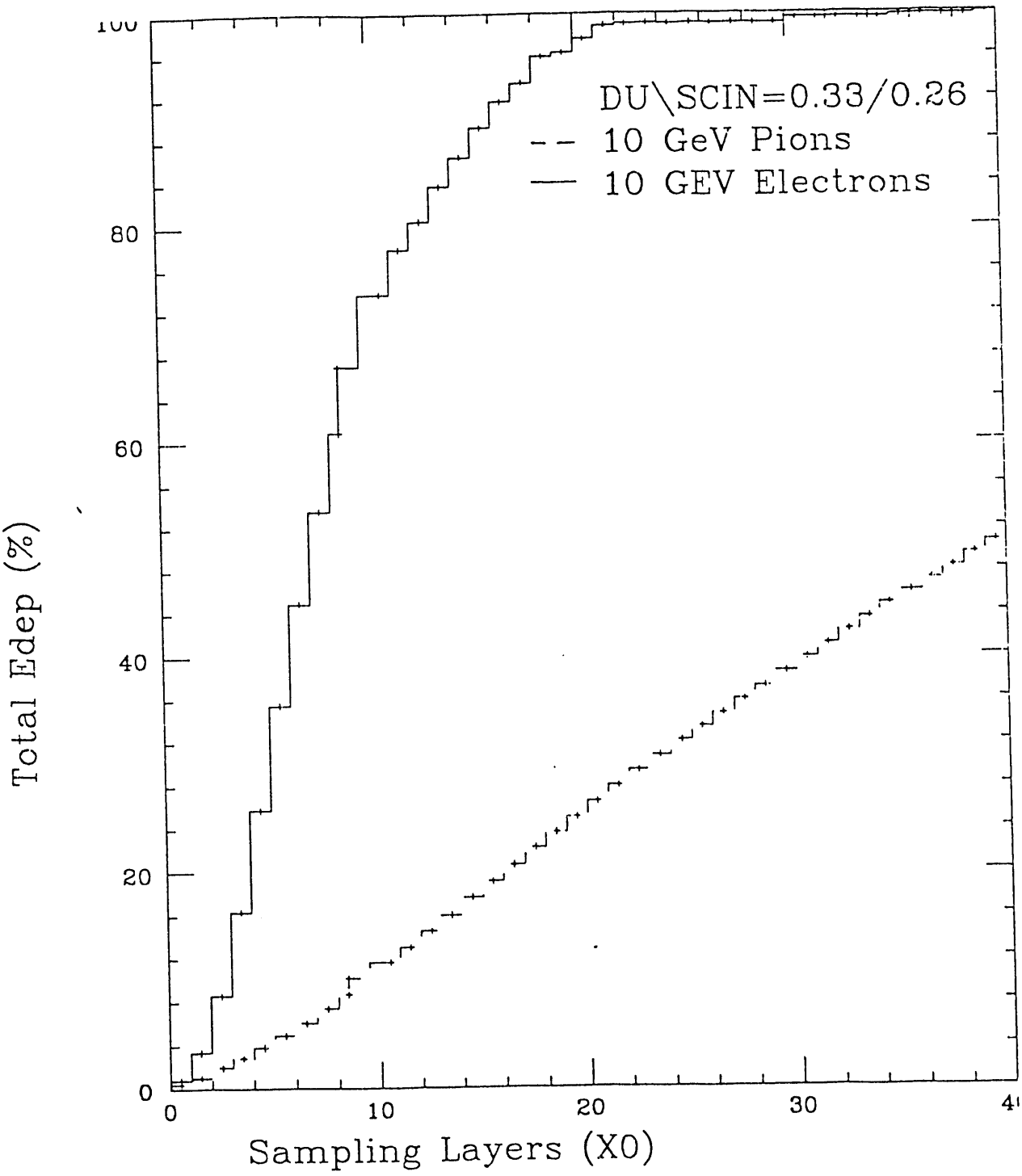
DU\SCIN=0.33/0.26
-- 10 GeV Pions
— 10 GEV Electrons
Total Edep (%)
Sampling Layers (X0)
0
20
40
60
80
100
0
10
20
30

FIG .21

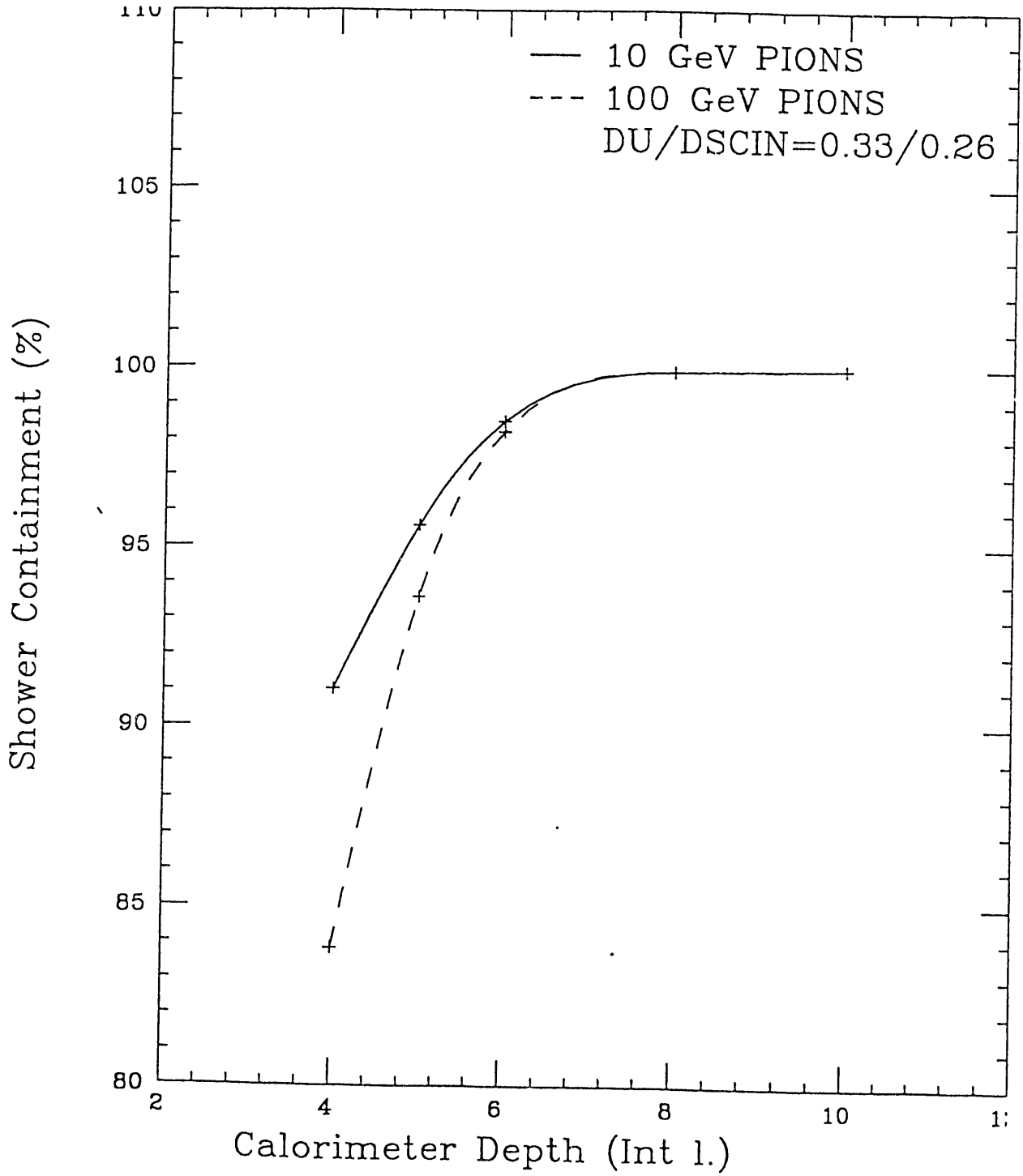
10 GeV PIONS
100 GeV PIONS
DU/DSCIN=0.33/0.26
Shower Containment (%)
110
105
100
95
90
85
80
2
4
6
8
10
Calorimeter Depth (Int l.)

FIG .22

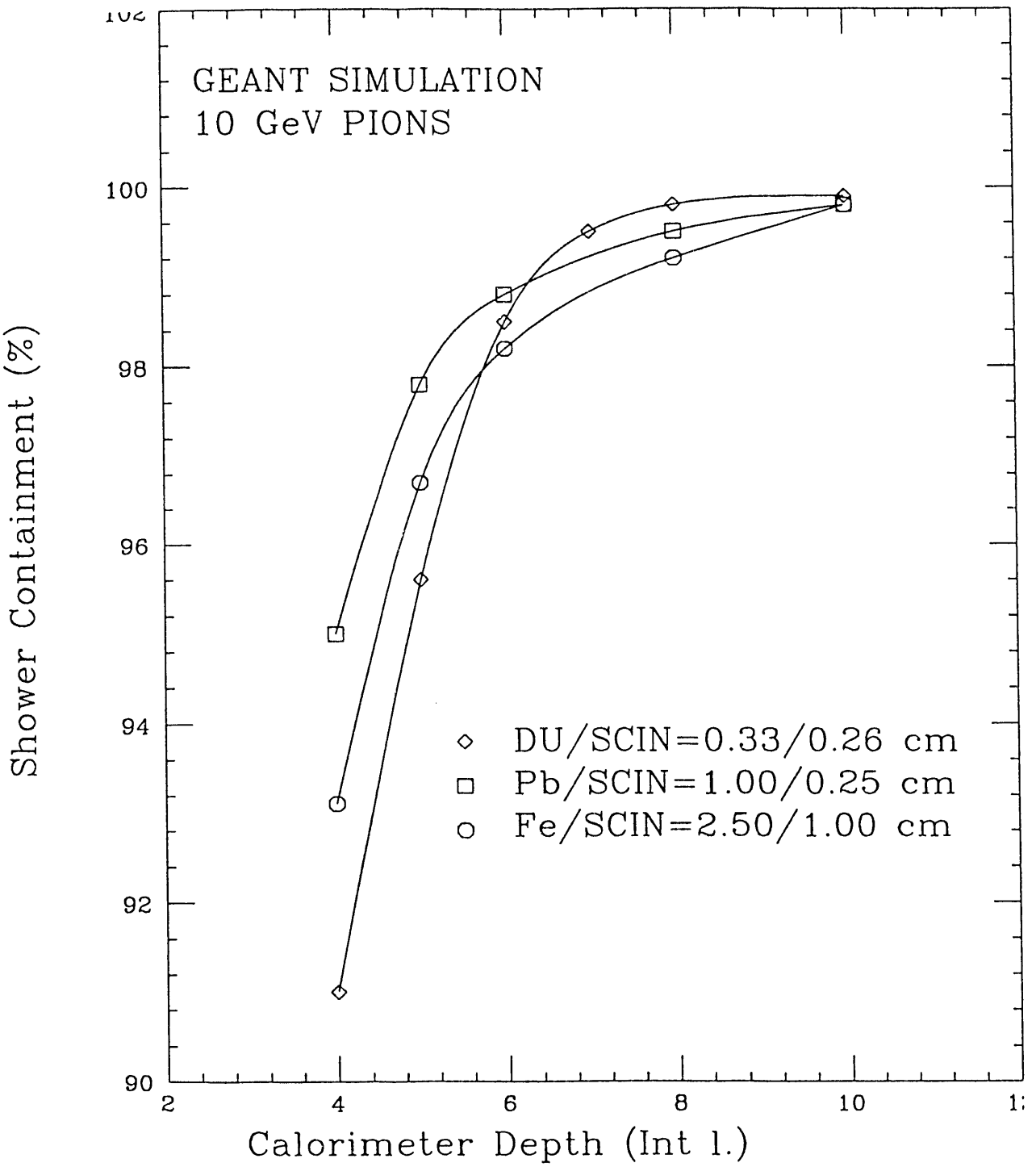
GEANT SIMULATION
10 GeV PIONS
Shower Containment (%)
Calorimeter Depth (Int l.)
DU/SCIN=0.33/0.26 cm
Pb/SCIN=1.00/0.25 cm
Fe/SCIN=2.50/1.00 cm
90
92
94
96
98
100
2
4
6
8
10

FIG .23

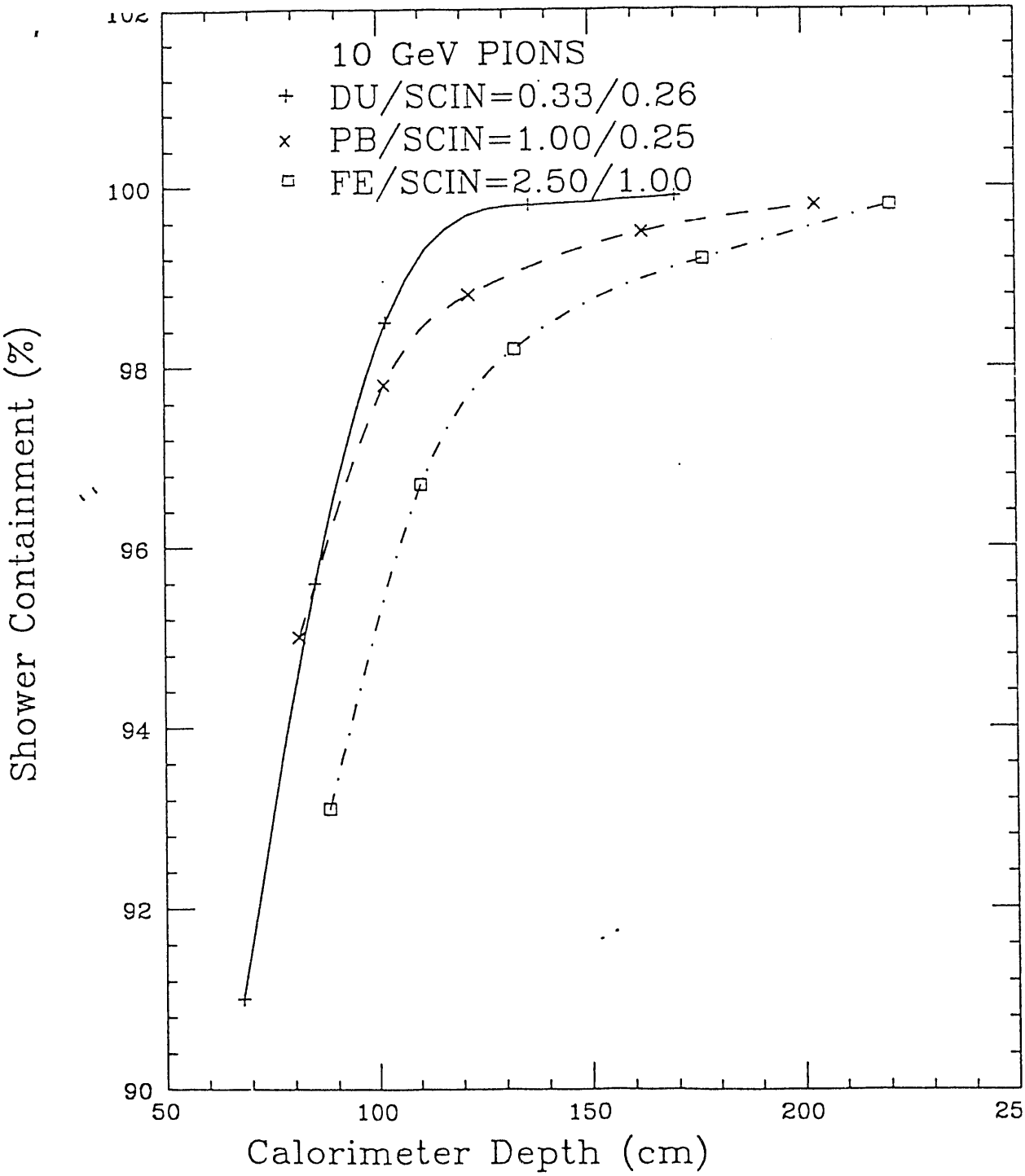
10 GeV PIONS
+ DU/SCIN=0.33/0.26
× PB/SCIN=1.00/0.25
□ FE/SCIN=2.50/1.00
Shower Containment (%)
Calorimeter Depth (cm)
90
92
94
96
98
100
50
100
150
200
25

FIG .23 A

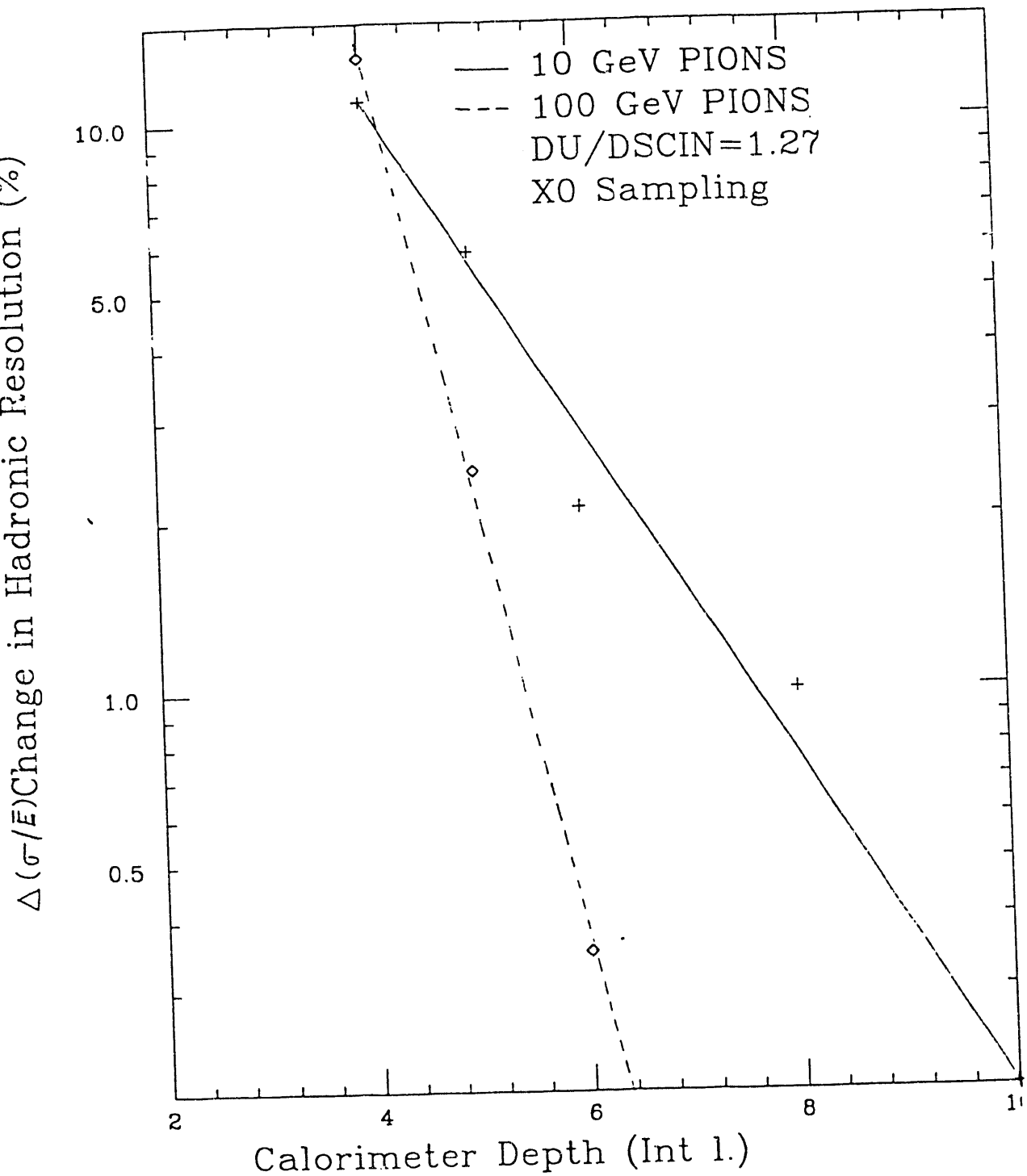
10 GeV PIONS
100 GeV PIONS
DU/DSCIN=1.27
X0 Sampling
10.0
5.0
1.0
0.5
2
4
6
8
Δ(σ/E)Change in Hadronic Resolution (%)
Calorimeter Depth (Int l.)

FIG .24

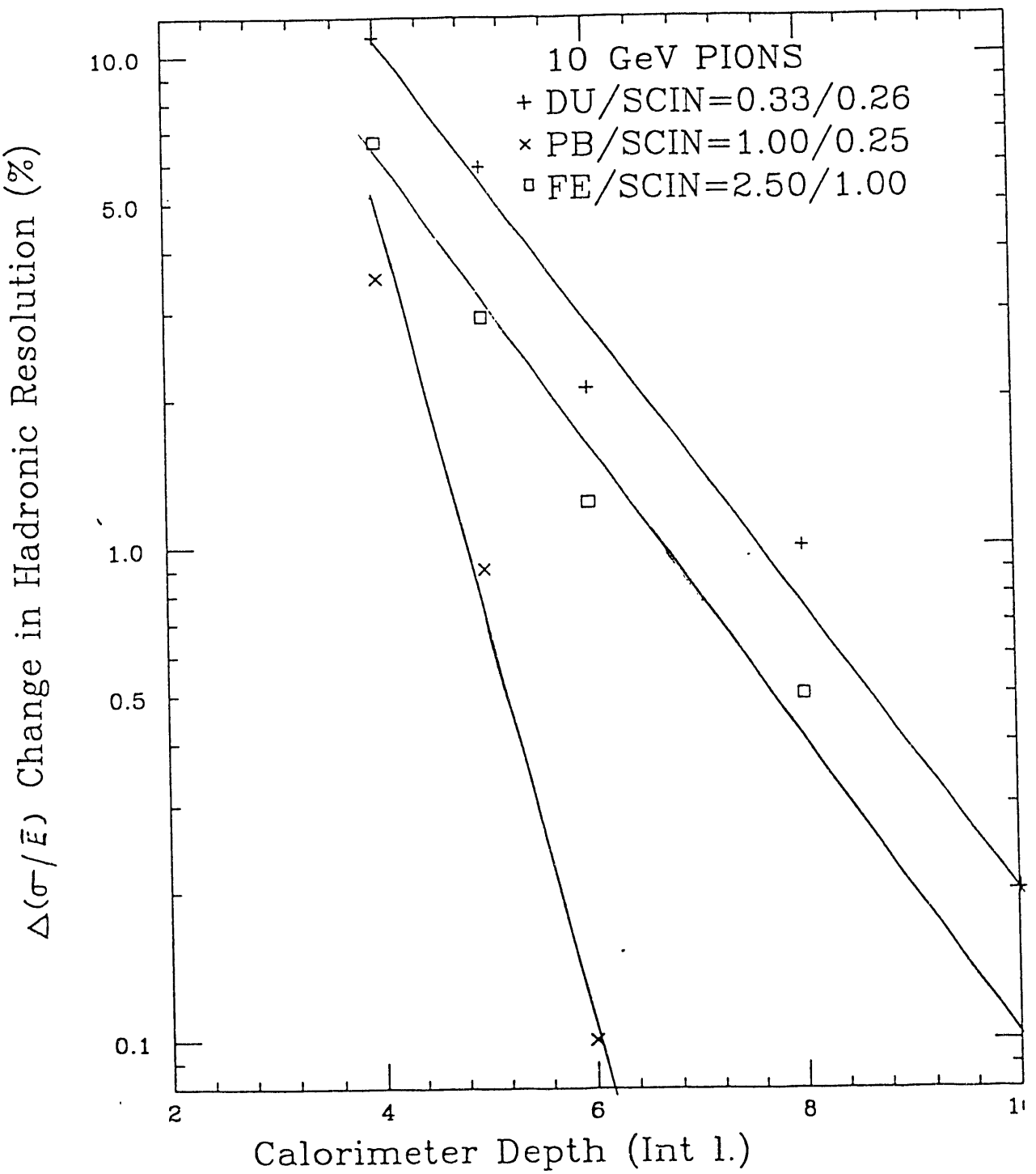
10 GeV PIONS
+ DU/SCIN=0.33/0.26
× PB/SCIN=1.00/0.25
□ FE/SCIN=2.50/1.00
10.0
5.0
1.0
0.5
0.1
2
4
6
8
Δ(σ/Ē) Change in Hadronic Resolution (%)
Calorimeter Depth (Int l.)

FIG .25

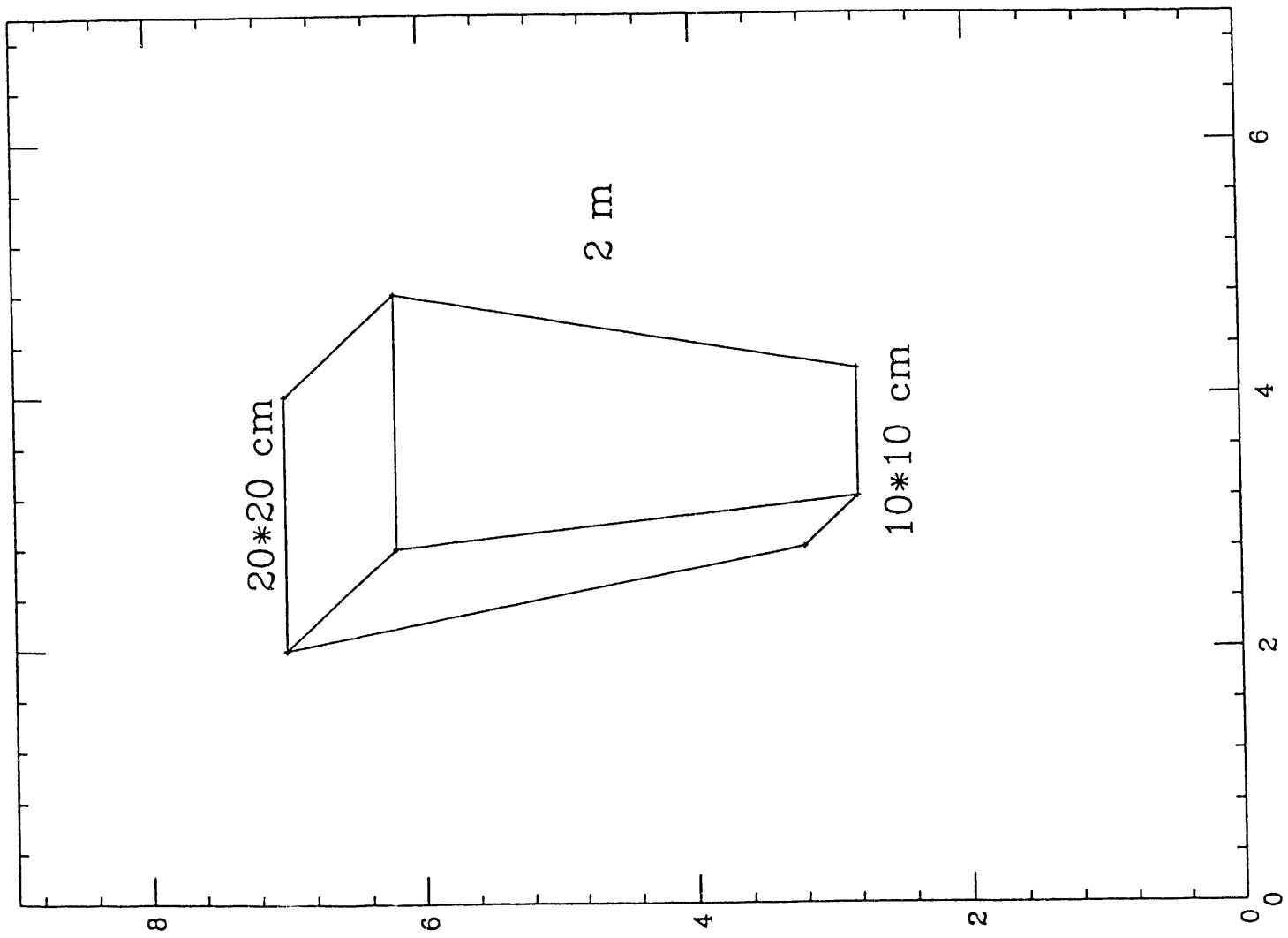

FIG .26

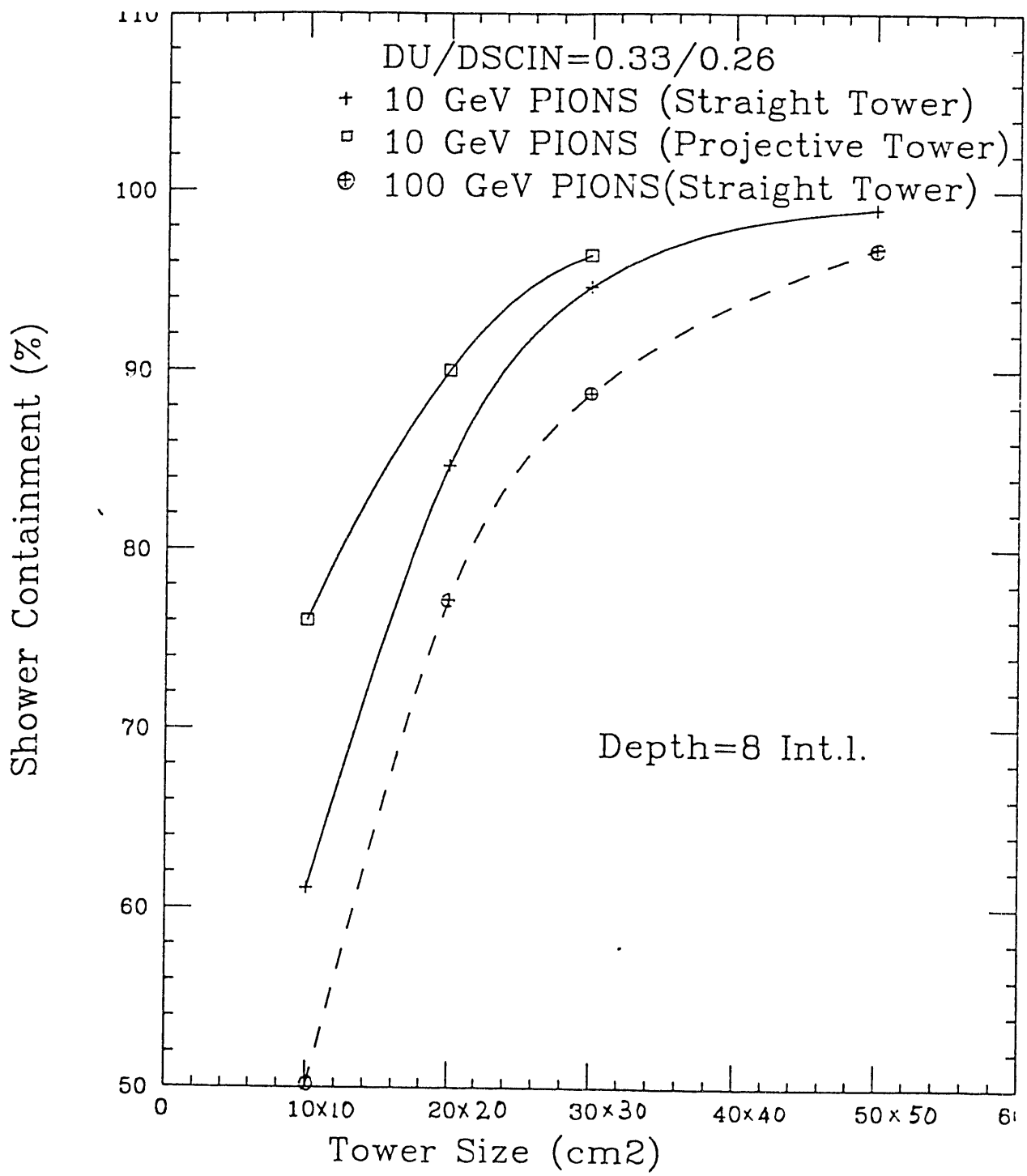
DU/DSCIN=0.33/0.26
10 GeV PIONS (Straight Tower)
10 GeV PIONS (Projective Tower)
100 GeV PIONS(Straight Tower)
Depth=8 Int.l.
Shower Containment (%)
Tower Size (cm2)
110
100
90
80
70
60
50
0
10x10
20x20
30x30
40x40
50x50

FIG .27

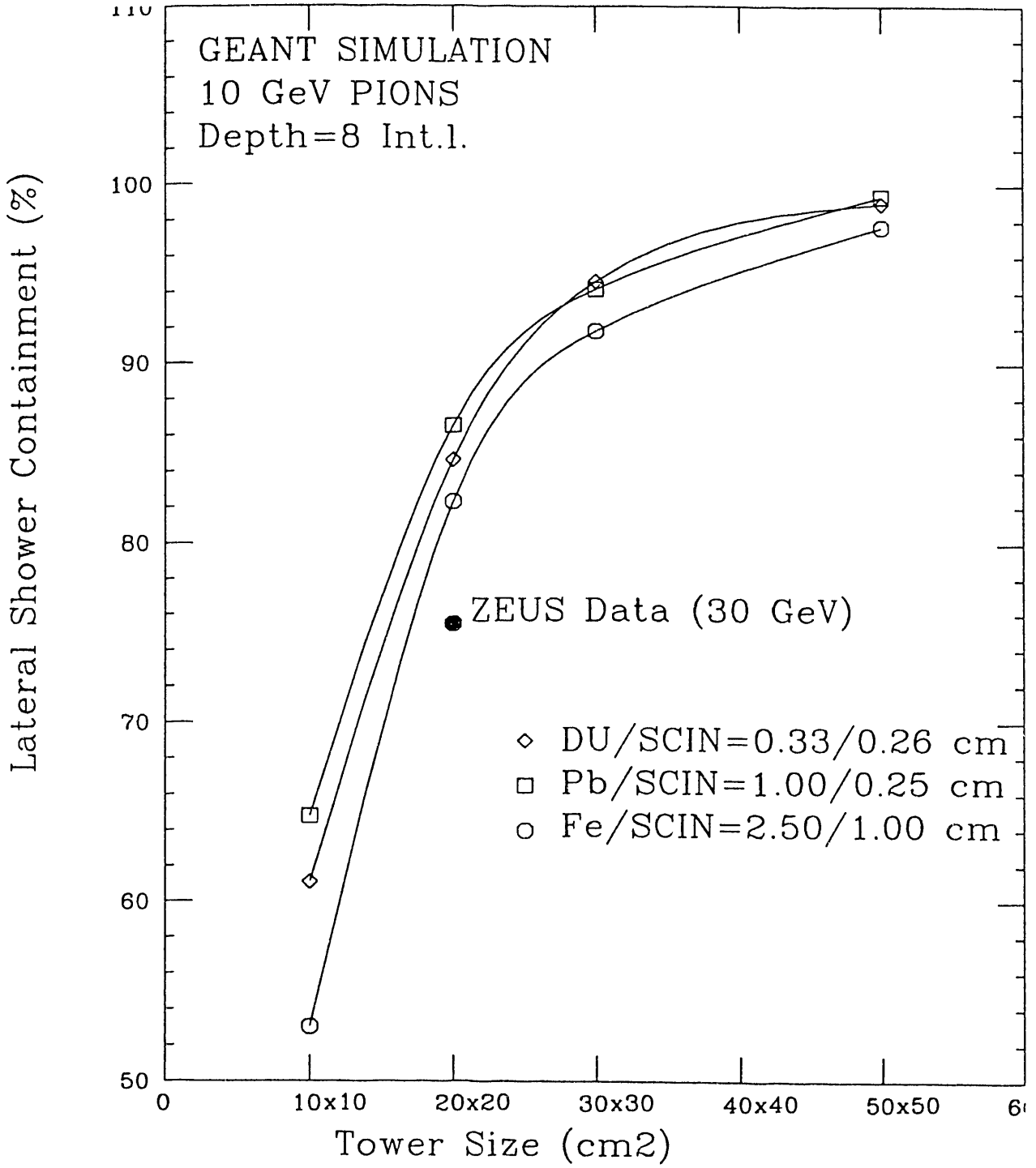
GEANT SIMULATION
10 GeV PIONS
Depth=8 Int.l.
Lateral Shower Containment (%)
110
100
90
80
70
60
50
0
10x10
20x20
30x30
40x40
50x50
Tower Size (cm2)
ZEUS Data (30 GeV)
DU/SCIN=0.33/0.26 cm
Pb/SCIN=1.00/0.25 cm
Fe/SCIN=2.50/1.00 cm

FIG .28

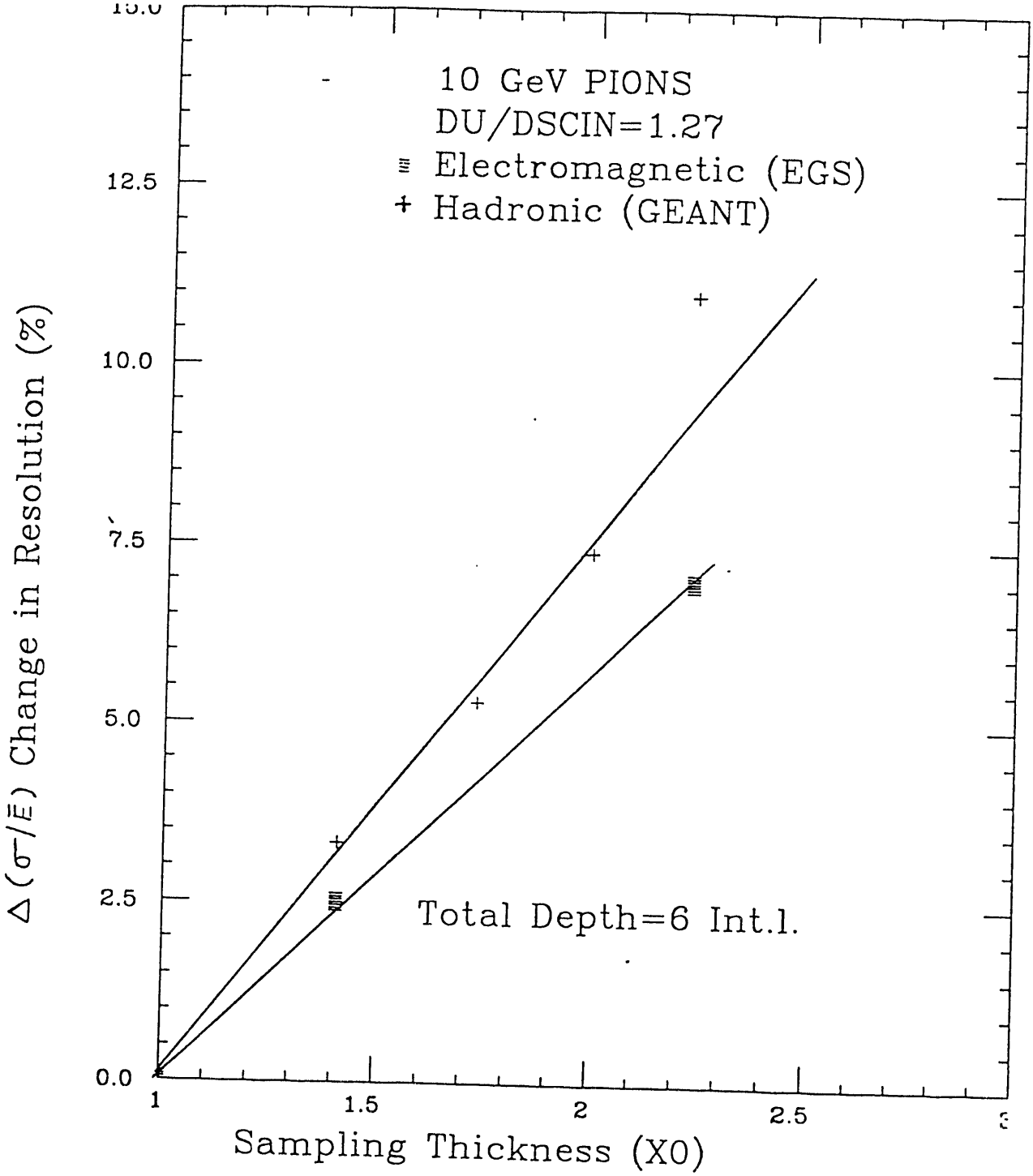
10 GeV PIONS
DU/DSCIN=1.27
Electromagnetic (EGS)
Hadronic (GEANT)
Total Depth=6 Int.l.
Δ(σ/Ē) Change in Resolution (%)
Sampling Thickness (X0)
0.0
2.5
5.0
7.5
10.0
12.5
1
1.5
2
2.5

FIG .29

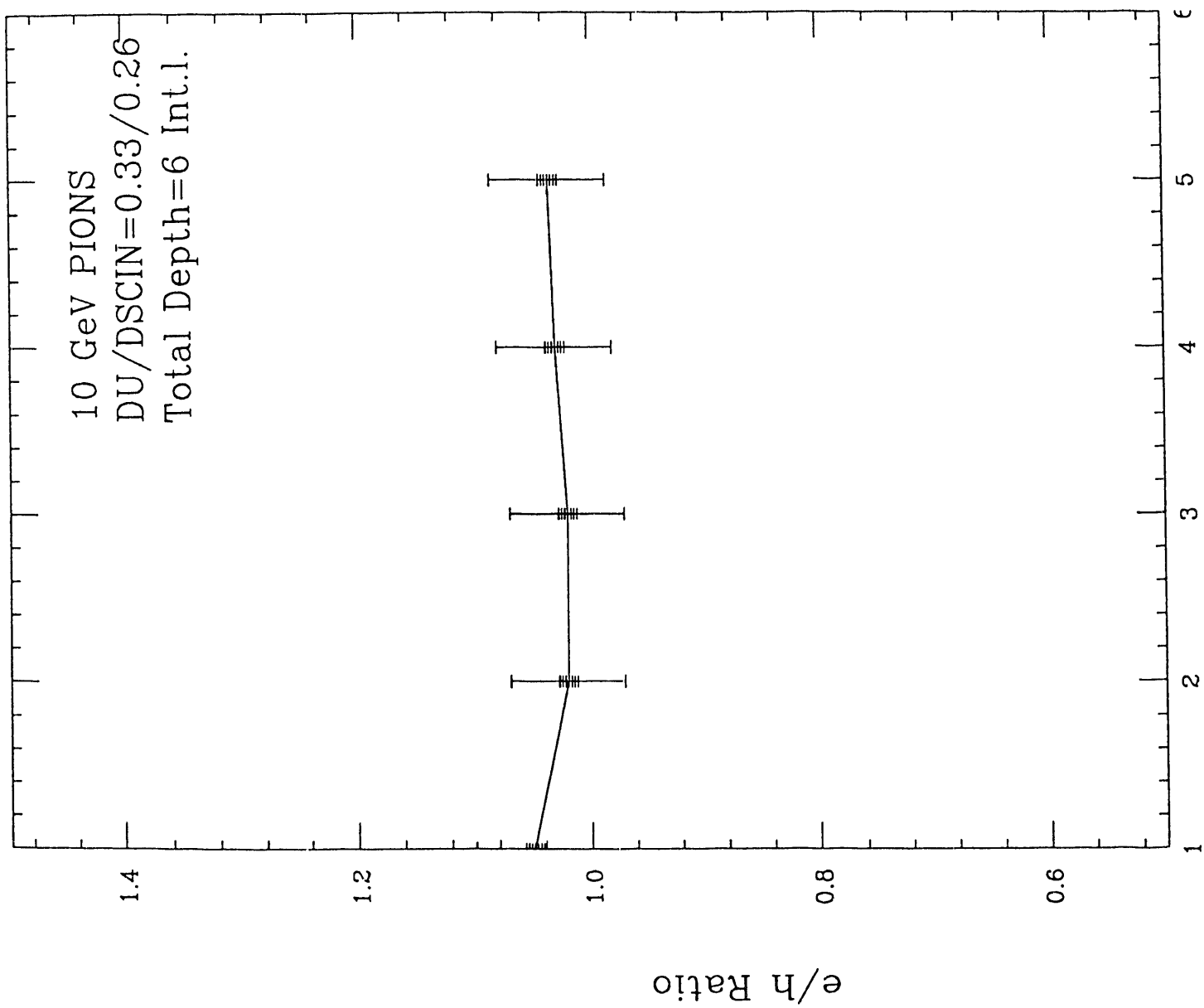
10 GeV PIONS
DU/DSCIN=0.33/0.26
Total Depth=6 Int.l.
e/h Ratio
1.4
1.2
1.0
0.8
0.6
1
2
3
4
5
Sampling Thickness (X0)

FIG .30

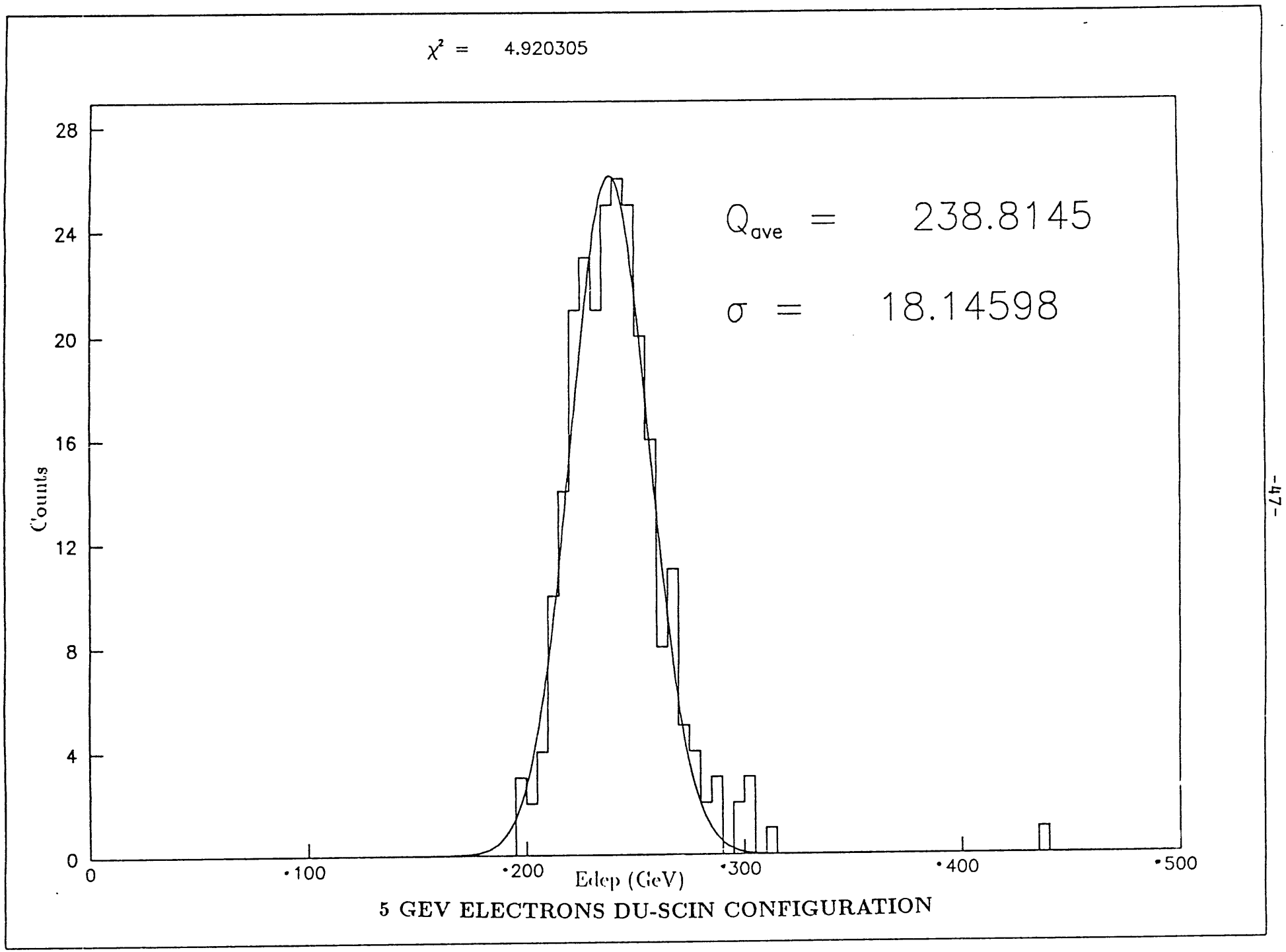
χ^2 = 4.920305
Q_{ave} = 238.8145
σ = 18.14598
Counts
Edep (GeV)
0
4
8
12
16
20
24
28
100
200
300
400
500
5 GEV ELECTRONS DU-SCIN CONFIGURATION

FIG .31

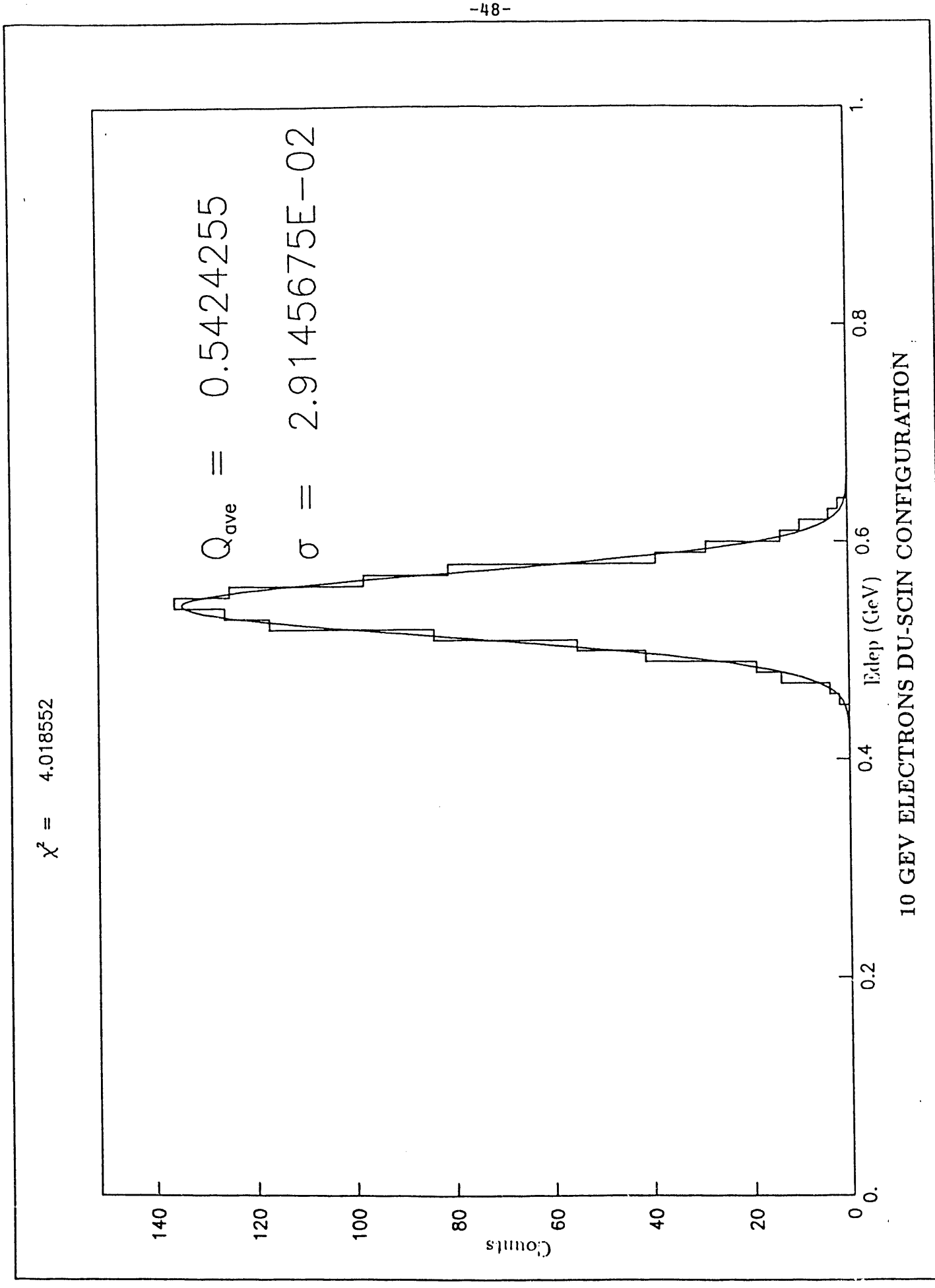
10 GEV ELECTRONS DU-SCIN CONFIGURATION
χ^2 = 4.018552
Q_{ave} = 0.5424255
σ = 2.9145675E-02
Counts
Edep (GeV)
0.
0.2
0.4
0.6
0.8
1.
0
20
40
60
80
100
120
140

FIG. 32

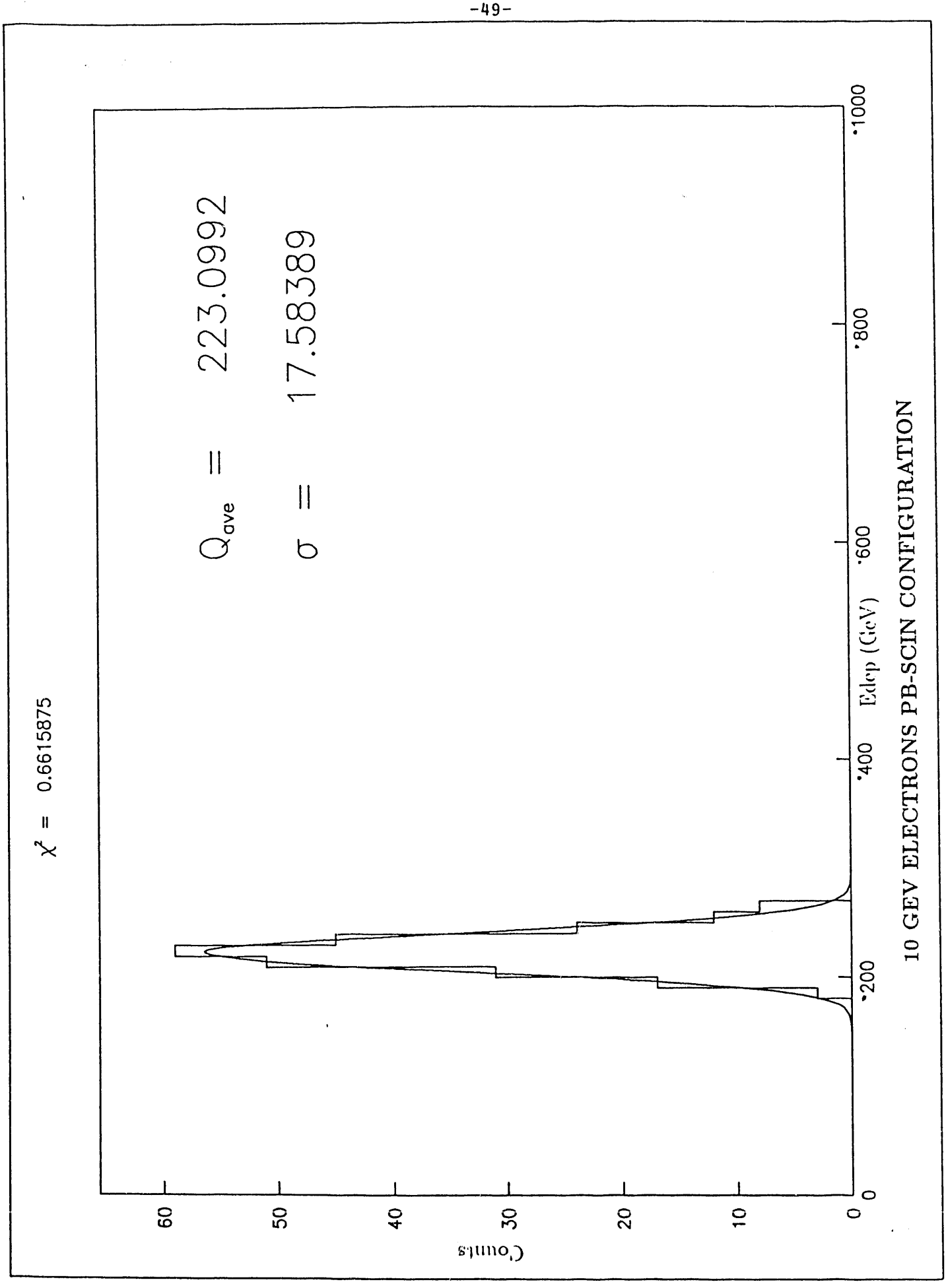
10 GEV ELECTRONS PB-SCIN CONFIGURATION
χ^2 = 0.6615875
Q_{ave} = 223.0992
σ = 17.58389
Counts
Edep (GeV)
0
10
20
30
40
50
60
200
400
600
800
1000

FIG .33

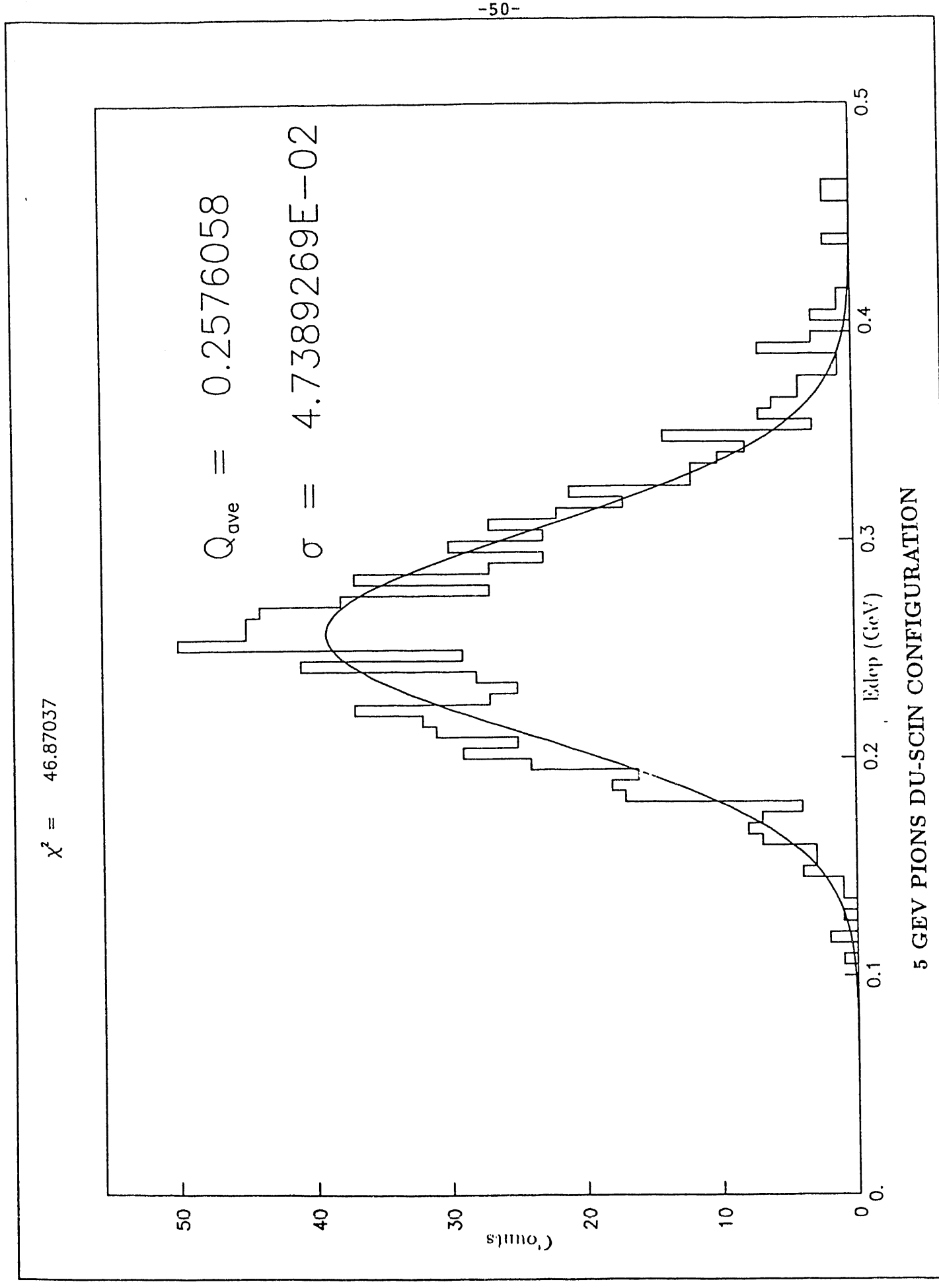
5 GEV PIONS DU-SCIN CONFIGURATION
Edep (GeV)
Counts
χ^2 = 46.87037
Q_{ave} = 0.2576058
σ = 4.7389269E-02
0.
0.1
0.2
0.3
0.4
0.5
10
20
30
40
50

FIG 31

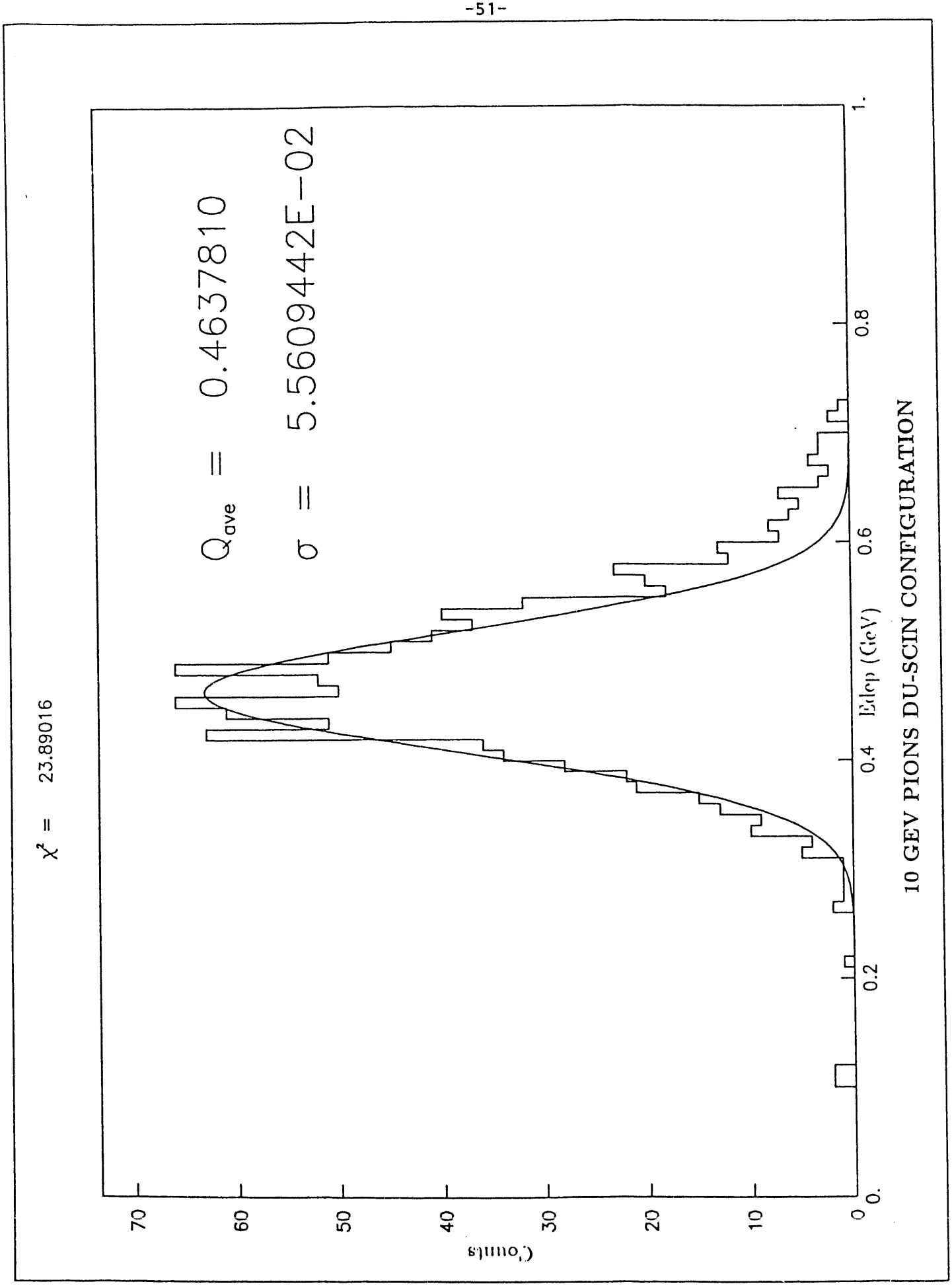
10 GEV PIONS DU-SCIN CONFIGURATION
χ^2 = 23.89016
Q_{ave} = 0.4637810
σ = 5.5609442E-02
Counts
Edep (GeV)
0.
0.2
0.4
0.6
0.8
1.
0
10
20
30
40
50
60
70

FIG .35

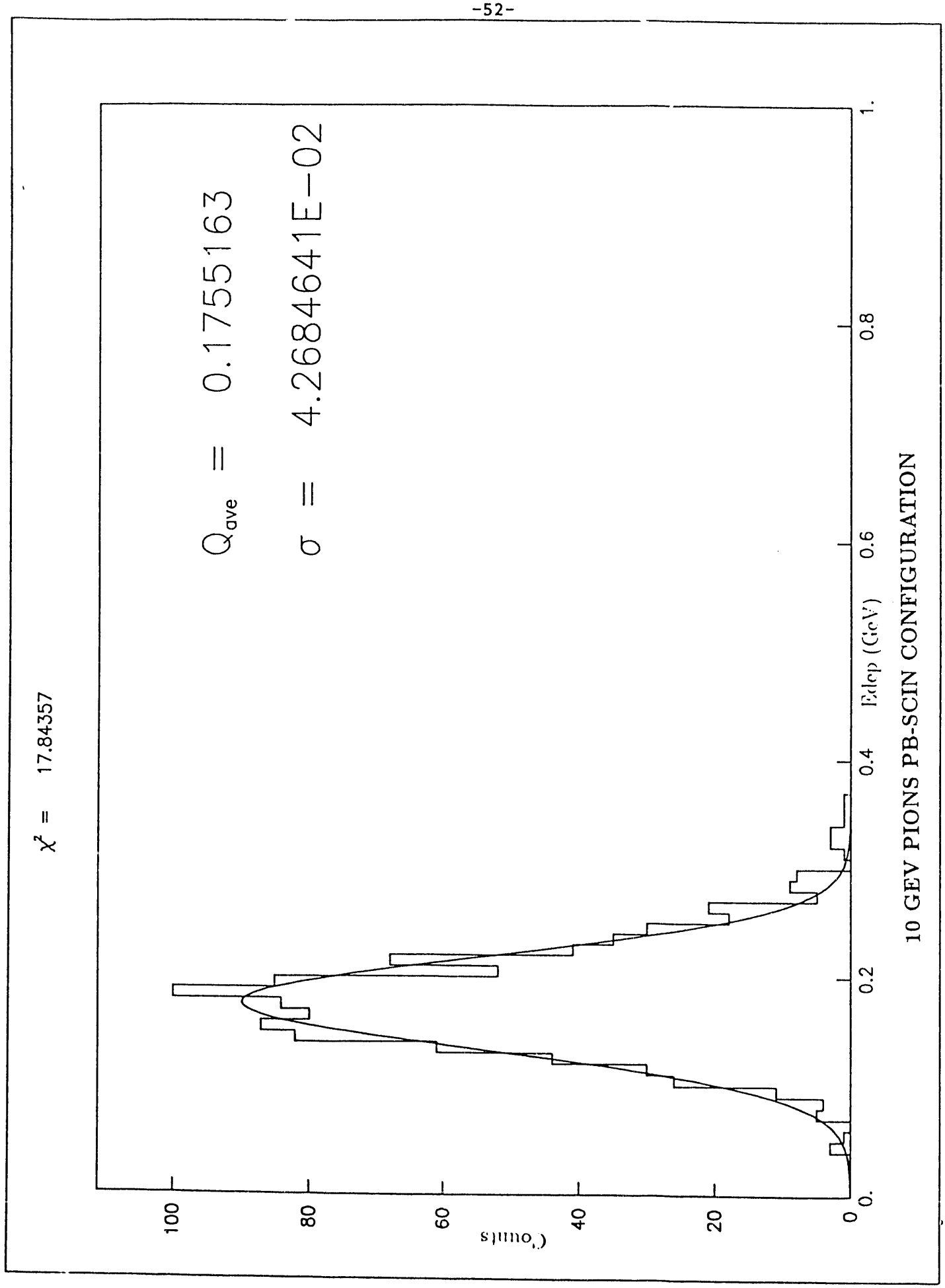
10 GEV PIONS PB-SCIN CONFIGURATION
χ^2 = 17.84357
Q_{ave} = 0.1755163
σ = 4.2684641E-02
Counts
Edep (GeV)
0.
0.2
0.4
0.6
0.8
1.
0
20
40
60
80
100

FIG. 36

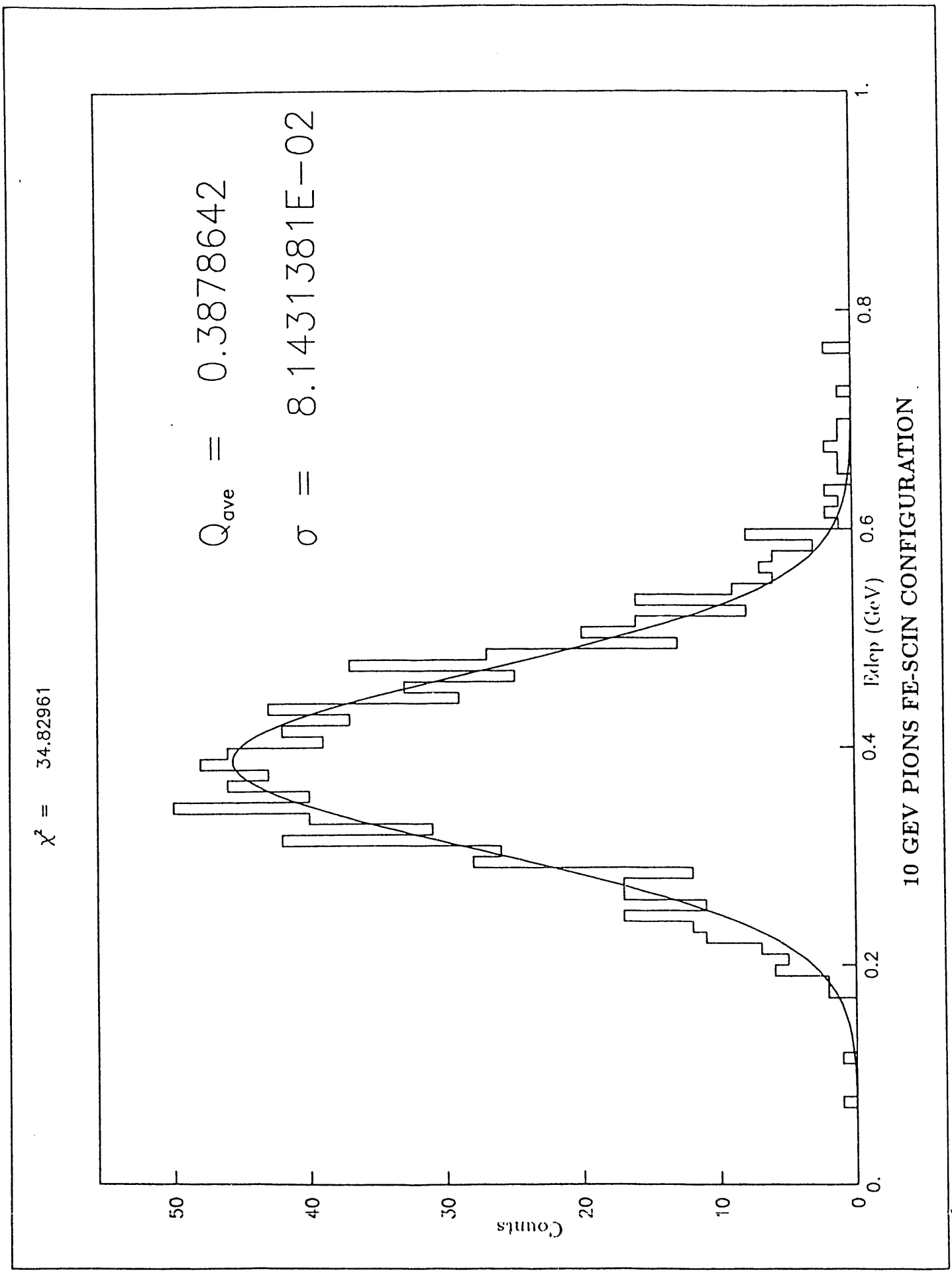
10 GEV PIONS FE-SCIN CONFIGURATION
χ^2 = 34.82961
Q_{ave} = 0.3878642
σ = 8.1431381E-02
Counts
Edep (GeV)
0.
0.2
0.4
0.6
0.8
1.
0
10
20
30
40
50

FIG .37

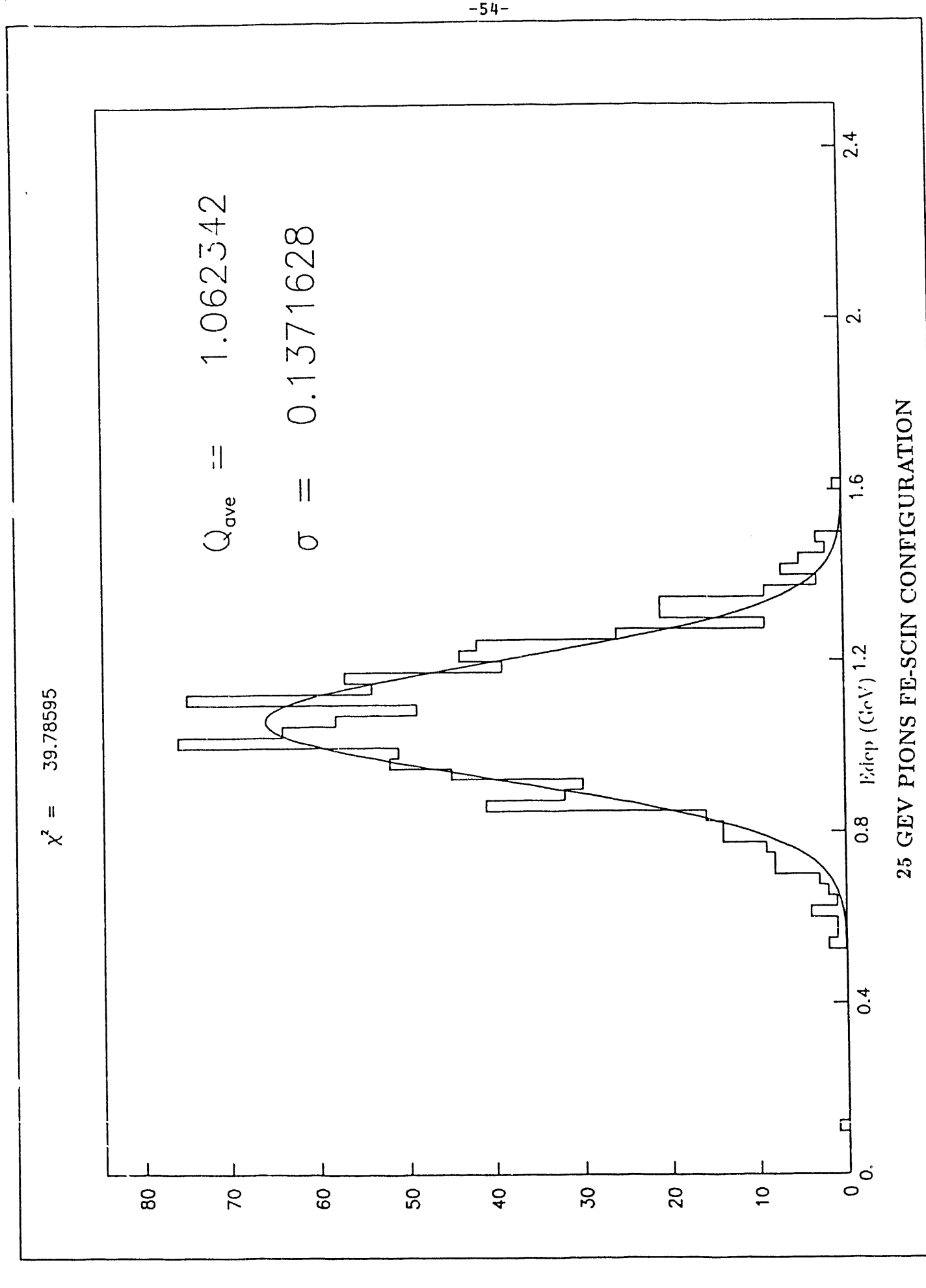
25 GEV PIONS FE-SCIN CONFIGURATION
χ^2 = 39.78595
Q_{ave} = 1.062342
σ = 0.1371628
Edep (GeV)
0.
0.4
0.8
1.2
1.6
2.
2.4
0
10
20
30
40
50
60
70
80

FIG 38

END

DATE
FILMED
11/16/93